

Review

Hail: Mechanisms, Monitoring, Forecasting, Damages, Financial Compensation Systems, and Prevention

Min Hee Kim ¹, Jaeyong Lee ² and Seung-Jae Lee ^{1,*}

¹ National Center for AgroMeteorology (NCAM), Seoul National University, Seoul 08826, Republic of Korea; mhkim@ncam.kr

² Geosystem Research Corporation, Gunpo 15807, Republic of Korea; jaeyl@geosr.com

* Correspondence: sjlee@ncam.kr; Tel.: +82-2-871-0236; Fax: +82-2-871-0230

Abstract: Hail has long caused extensive damage and economic loss in places inhabited by humans. Climate change is expected to lead to different types of damage due to the geographic characteristics of each continent. Under changing environment, hail is becoming increasingly unstable and is causing damage that is difficult to repair, making it essential to study the occurrence of hail and hail-damage. Hail formation has been studied at the micro- and macrophysical scales as well as thermal and dynamical scales. Hail forms in various sizes, and the scale of damage varies with size. Hail precipitation occurs suddenly and is localized, making it difficult to observe and predict. Nonetheless, techniques to measure and forecast hail precipitation are improving in accuracy. Hail-damage management and financial compensation systems are used to mitigate the severe economic losses caused by hail fallen in rural and urban areas. This review most comprehensively considers hail research, focusing on the mechanisms, observation and prediction methods, damage, social compensation systems for hail damage, and hail-disaster prevention, suggesting future study directions briefly.

Keywords: hail mechanisms; hail forecasting; hail damage; hail compensation system; hail prevention



Citation: Kim, M.H.; Lee, J.; Lee, S.-J. Hail: Mechanisms, Monitoring, Forecasting, Damages, Financial Compensation Systems, and Prevention. *Atmosphere* **2023**, *14*, 1642. <https://doi.org/10.3390/atmos14111642>

Academic Editors: Tomeu Rigo, Anthony R. Lupo and John Walsh

Received: 15 August 2023
Revised: 29 September 2023
Accepted: 16 October 2023
Published: 31 October 2023



Copyright: © 2023 by the authors. Licensee MDPI, Basel, Switzerland. This article is an open access article distributed under the terms and conditions of the Creative Commons Attribution (CC BY) license (<https://creativecommons.org/licenses/by/4.0/>).

1. Introduction

Climate change is progressively becoming a more serious global issue, causing extreme temperatures, wildfires, droughts, heavy precipitation, floods, and the glacial reduction [1]. Hail precipitation, or hails, are affected by climate change [2–8]. It is reported in Raupach et al. [6] that the small scale and relatively rare nature of hailstorms make them challenging to model, but climate change is likely to impact hail formation (impacting low levels of moisture, convective instability, microphysical processes, and vertical wind shear) and properties. Anthropogenically enhanced greenhouse gas concentrations affects the frequency and intensity of hail with dependency on a range of physical processes and scales [9]. Trends in hail precipitation vary between continents [2,4,7,10,11]. Hail involves the sudden and localized precipitation of ice, making hail events difficult to sample and study, and current hail analysis techniques have many limitations [11,12]. Unexpected localized hailstorms can cause enormous physical and economic damage, harming people and damaging accommodation, crops, vehicles, windows, solar panels, roofs, walls, and agricultural products [13–17].

Hail frequency varies between the continents under changing climate scenario (Figure 1), and the trends have been divided into three categories [4]. In North America, large hailstones are increasingly likely to form; in Europe and Australia, hail precipitation frequency has increased; in South America, hail precipitation events have become less severe in the warm and humid parts; and in Asia, hail precipitation events have become less frequent, although hail precipitation event size has remained unchanged [18]. Areas with high hail frequency are typically $\pm 30^\circ$ from the equator [19]. In addition, it can be

seen that the frequency of hail is high in places where there is a clear contrast between land and sea in terms of hail formation [19]. Prominent examples include the Rocky Mountains, the Andes, the southern foothills of the Himalayas, and the mountains of Central Africa and the Arabian Peninsula [19]. Conversely, areas with low hail frequency are poleward of $\pm 60^\circ$ [19]. Additionally, the east side of the continent generally has a higher risk of hail than the west [19].

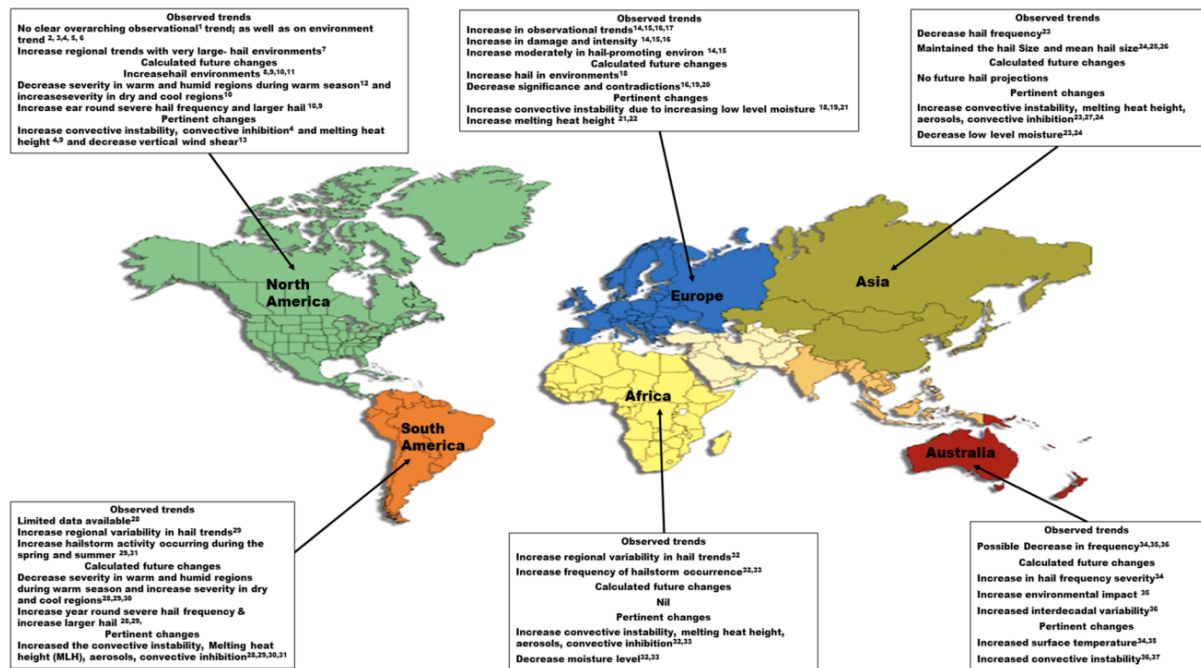


Figure 1. Global assessment of hail occurrence under changing climate scenarios. Taken from [1–37].

According to the European Severe Weather Database (ESWD), large hail was observed in Vienna, Austria in the 1960s, but large hail was observed throughout Central Europe in the 1970s. Since the 1980s, the area where large hail occurs has expanded from Western Europe to Eastern Europe, and from the 1990s to the 2020s, the area and frequency of large hail are observed to have intensified. The ESWD data shows that the frequency of large hail increases as time passes. Although the frequency of large hail has increased, hail observations have become more sophisticated as technology has improved. As more and more such large hails are discovered, greater damage is caused to people, which leads to intensifying research as well.

We searched for articles containing the keywords “hailstone instrument”, “hailstone forecasting”, “hailstone detection”, and “hailstone damage” published up to 14 September 2021 (Figure 2): the number of hail-related articles has increased, with “hailstone damage” fetching the most results, followed by “hailstone instrument”. Notably, in the 1980s, fewer papers were registered for “hailstone forecasting” than for “hailstone detection”.

When searching in Scopus using the words searched in Google Scholar, it was confirmed that the results for hailstone damage were overwhelmingly high (Figure 3). Similarly, there was a slight difference between hailstone forecasting and hailstone detection, but the number of retrieved papers was similar. The common field of research for the four search terms was identified as Earth and Planetary Sciences. Hailstone-related research is steadily progressing in the fields of environmental science and computer science.

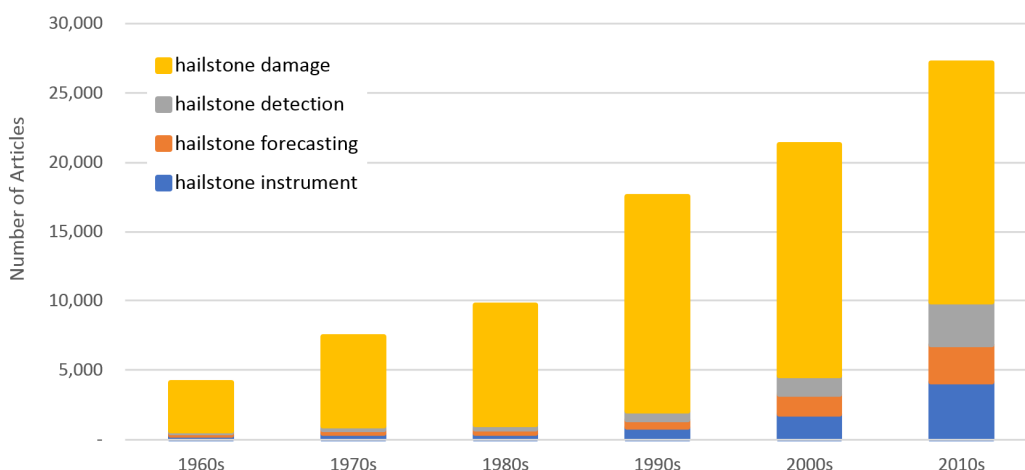


Figure 2. Articles published on hail-related topics up to 14 September 2021, using a Google Scholar search.

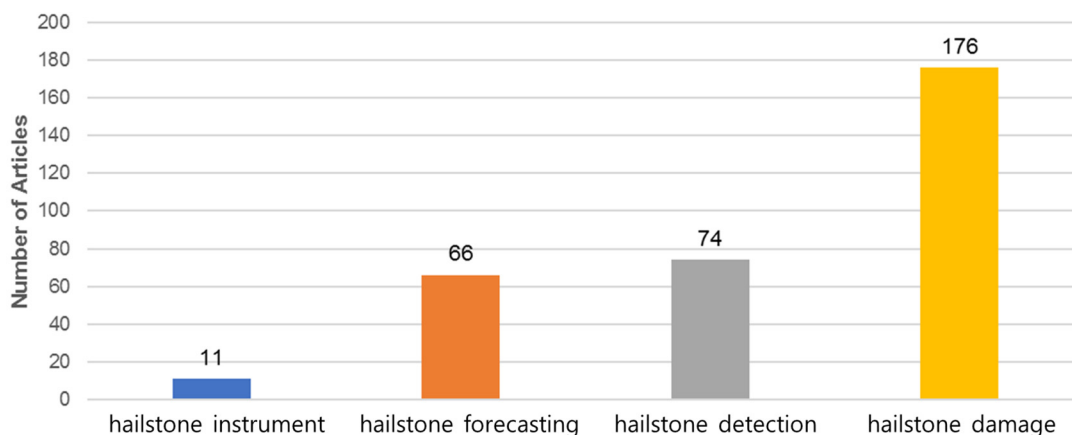


Figure 3. Articles published on hail-related topics up to 19 September 2023, using a Scopus.

Although a Google Scholar and Scopus search returned articles addressing each of these aspects separately, few studies have addressed them simultaneously. Although disaster-prevention tools based on hail-formation mechanisms have been developed, hail continues to cause damage, with the effects varying between continents. The present review paper aims to address this by comprehensively considering and integrating hail research, focusing on the mechanisms, observation and prediction methods, damage, compensation systems for hail damage, and hail-disaster prevention. Section 2 describes the properties of hail, including the conditions and process of its formation and its composition. Sections 3–7 describe, respectively, observation methods, prediction methods, hail-related damage, hail-damage compensation systems, and physical and chemical containment methods to reduce hail damage.

2. Mechanisms of Hail Formation

Thunderstorms are local storms invariably produced by cumulonimbus clouds, which nearly always generate hail, as well as lightning, thunder, strong gusts of wind, and heavy rain. Thunderstorms have the developing stage, the mature stage, and the dissipating stage. The developing stage of a thunderstorm is marked by a cumulus cloud that is being pushed upward by an updraft and soon looks like a tower (called towering cumulus) as the updraft continues to develop. There is little to no rain during this stage but occasional lightning. The thunderstorm enters the mature stage when the updraft continues to feed the storm, but precipitation begins to fall out of the storm, creating a downdraft. When

the downdraft and rain-cooled air spreads out along the ground it forms a gust front. The mature stage is most favorable to hail formation (Figure 4a). Thunderstorms have several different types such as single cell, multi-cell, super-cell, meso-scale convective complexes, squall lines, derechos, etc. The NOAA website says that super-cell thunderstorms are perhaps the most violent of all these thunderstorm types, and are capable of producing large hail, and even weak-to-violent tornadoes. However, other thunderstorm types are also known to produce small hail (ice pellets or snow pellets) to large hail with different duration time. Figure 4a shows thunderstorm clouds. (1) A shelf cloud is a long wedge shape cloud that forms on the leading edge of a squall line or multi-cluster storm system. Shelf clouds are visually dramatic and indicate an approaching storm, however they do not always appear during the most severe weather phenomena such as large hail. (2) Wall clouds, particularly those within supercell thunderstorms, are rotating and often observed in the vicinity of large hail. (3) A funnel cloud is a cone-shaped cloud which extends from the base of a towering cumulus towards the ground without actually reaching the surface (and hence different from a tornado), and is less conducive to hail.

Micro- and macrophysics play important roles in hail formation and growth. Micro-physically, hail formation and growth require small particles that act as nuclei, supercooled water droplets, and sufficient growth time [17,20–23]. First, small nucleus-serving particles, <1 mm in diameter, aggregate to form an ‘embryo’ (i.e., an ice crystal) comprising graupel (consisting of snow particles <5 mm in diameter) or frozen droplets [21,24]. These small particles ascend and descend within clouds on air currents [21]. Supercooled water droplets, which are essential for hail growth [20–23], then attach to the embryo and freeze, either immediately (known as riming) or shortly thereafter (known as accretion) [21]. Hailstone growth requires graupels and supercooled droplets to exist simultaneously. Hailstones grow most actively when the supercooled water droplets are at temperatures from -10 to -25 °C, although they continue to grow at supercooled water droplets temperatures as low as -38 °C, the homogeneous freezing temperature of water [25–27]. Hail growth requires sufficient time [17,20–23] for the embryo to grow in the hail-growth zone where many supercooled water droplets are present [21,26–28]. Hail requires at least 10 min to achieve significant growth [26].

Optimal hail growth is dependent on several key characteristics [28]. For a hailstorm, thermal and dynamic factors play different role for its development, even the microphysics determine the macrophysical response [30]. Hail can be produced in all types of deep convective storms, from single-cell ordinary thunderstorms to supercells, and most large hail forms in multicellular or supercell convection [31]. In the case of cumulonimbus clouds (deep convective storms) that produce hail, there are single cell, multicell, MCCs (Mesoscale Convective Cloud systems), and supercells. Among these, hail is frequently generated in supercells [17,20,32]. And during the maturation process, which is a relatively early stage in the development of cumulonimbus clouds, hail within the cloud grows and falls to the ground [33].

Hailstone formation and growth (Figure 4) can occur only within the 60% of cumulonimbus clouds that can produce hail [34]. Hail forms at atmospheric pressures of 850–350 hPa, and is carried upward by strong updrafts. The air in these clouds condenses to form embryos that become seeds on which hail can grow [34,35]. Supercooled water droplets occur in the cumulonimbus cloud layers at temperatures between -10 and -40 °C [36]. As the embryo repeatedly ascends and descends, the ice crystals melt and freeze, causing gradual growth [34,37]. Conversely, hail may grow by slow rise or horizontal movement in a rising area rather than repeated rise and fall [20,38]. What the above two hail growth processes have in common is that they stay for a long time in the updraft area within the convective cloud [20,34,37,38]. When the terminal velocity of the hailstone becomes greater than the ascent velocity within the cumulonimbus cloud, or if it encounters downdrafts, it will fall to the ground, causing hail precipitation [34]. At this time, it was reported through trajectory analysis of numerical experiments that hail fell around the west or north side of the rising zone of cumulonimbus clouds [28,39,40]. It has been found optimal hail growth

may depend on complex hailstone pseudotrajectory with multiple ups and downs from numerical simulation [28], while a recent lab and numerical result only present a one-time up and down for a huge hailstone [29].

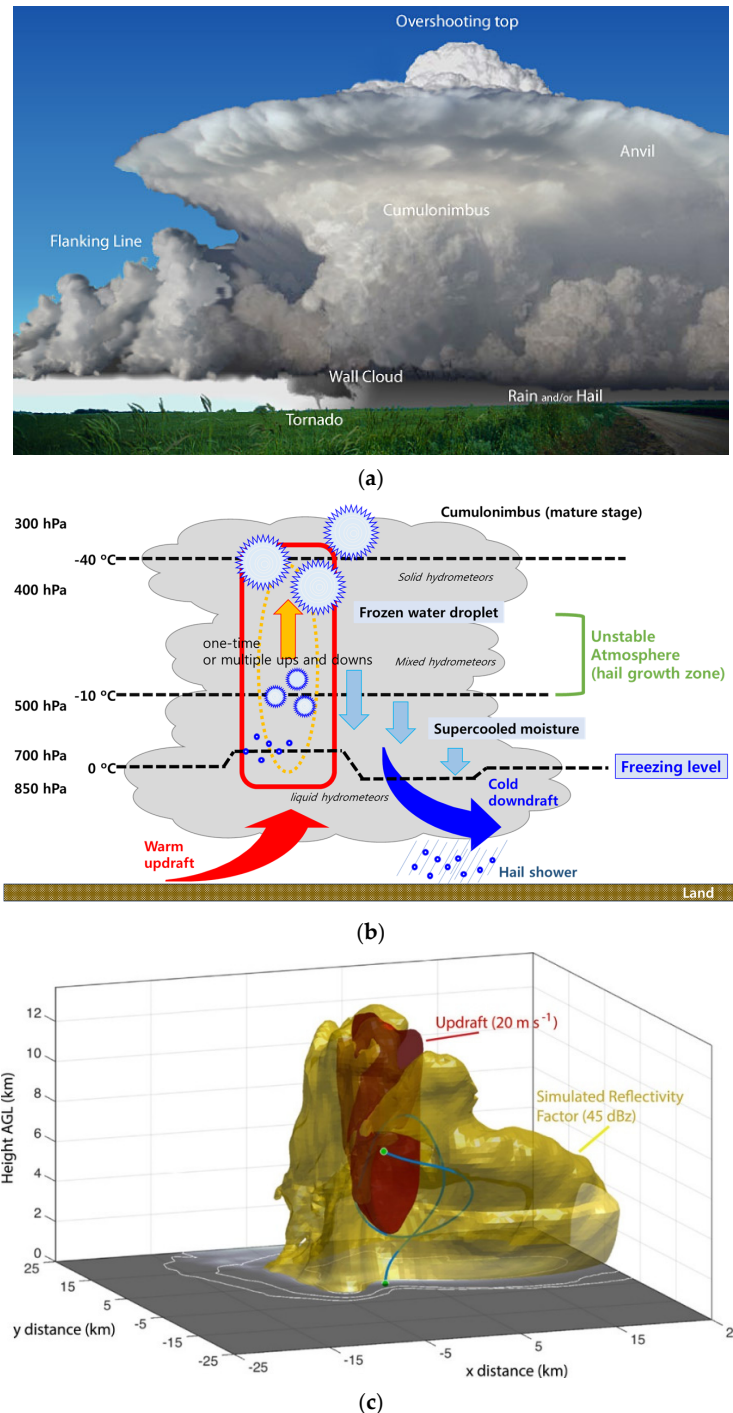


Figure 4. (a) An idealized supercell thunderstorm. Taken from the NOAA website <https://www.noaa.gov/jetstream/tstrmtypes> (accessed on 24 October 2023). (b) A simplified schematic of hail formation and growth at a mature stage of cumulonimbus clouds. Source: Own illustration. (c) Simulated hailstone pseudotrajectory (blue line) initialized as a 2-mm embryo (green circle) with the lowest model level 30-, 40-, and 50-dBz reflectivity factor (white contours) at the surface. Source: Taken from [29].

High levels of atmospheric instability, high liquid moisture content in clouds, low freezing temperatures, and high vertical wind shear provide the optimal and necessary conditions for hail formation. These optimal conditions increase the probability that hail will form [41,42]. Hail formation is always accompanied by the intersection of warm and cold fronts [43]. In the presence of hot air, the relatively dense cool air moves toward the less dense hot air, lifting it and destabilizing the atmosphere. This interaction forms a cumulonimbus cloud, which descends with thunder, lightning, and hail [15,44]. Hail arises when there are large temperature differences within the clouds, mainly in coastal and mountainous areas [43]. In the USA, for example, 41% of recorded hail events have occurred due to unstable air masses [44]. In South Korea, the cold and dry Siberian air and hot and humid North Pacific air masses meet, destabilizing the air and causing hail precipitation [15].

Hail is also generated in the mid-dry zone [45–47], at an altitude of 500–700 hPa, at which high density cold dry air enters the middle layer of the cumulonimbus cloud; the atmosphere then becomes unstable as wet air surrounded by low-density air is drawn in. This instability promotes updrafts, which increases the vertical motion of the ice masses. Thereafter, a strong downdraft is created with cold air flowing in, generating heavy precipitation and hail [45,46]. In this mid-dry zone, there is a significant difference in humidity between the upper and lower atmosphere [45–47]. Additionally, large CAPEs (Convective Available Potential Energy) and small CINs (Convective INhibition) may result in strong convection, generating in hailstones [48]. Finally, large SRH (Storm-Relative Helicity) and high wind shear are conducive to hail formation, as they induce updrafts [18,28,49].

3. Hail Observation

Hails causes economic losses to agriculture, forestry, and property such as buildings, vehicles, roads, and solar panels [41,50], with crop damage causing the largest category [50–53]. While hailstone size is an important factor in hail-related crop losses, hailstone density is also directly related to the extent of damage [51–53]. Good visibility is required to observe hail effectively. Hailstone diameter and width must be considered [51–53]. The National Oceanic and Atmospheric Administration (NOAA) uses 11 diameter-based sizes categories, each with an associated degree of damage (Table 1, Figure 5) [54].

Table 1. Hail intensity and magnitude.

Intensity	Size Category	Diameter (mm)	Shape	Impact
Hard hail	H0	<8.4	Pea	No damage
Potentially damaging	H1	8.4–15.2	Marble	Slight damage to plants, crops
	H2	15.2–20.3	Coin or grape	Substantial destruction to fruit, vegetation
Severe	H3	20.3–30.5	Nickel to quarter	Severe harm to fruit and yields, harm to glass and plastic structure
	H4	30.5–40.6	Golf ball	Extensive glass damage, vehicle-frame destruction

Table 1. Cont.

Intensity	Size Category	Diameter (mm)	Shape	Impact
Destructive	H5	40.6–50.8	Tennis ball	Extensive demolition of glass; destruction of tiled roofs; substantial risk of injury
	H6	50.8–61.0	Baseball	Aircraft body spoilt; walls ruttled
Very destructive	H7	61.0–76.2	Grapefruit	Severe roof destruction, risk of severe injury
	H8	76.2–88.9	Softball	Severe destruction to aircraft bodywork
Super hailstorms	H9	88.9–101.6	Softball	Extensive structural destruction, risk of severe or even fatal injury to persons caught in the open
	H10	>101.6	Softball and up	Extensive structural damage, risk of severe or even fatal injury to persons caught in the open

Data from: www.noaa.gov (accessed on 10 June 2021).



Figure 5. Hailstones generated by hailstorms of varying intensities. Data from: www.noaa.gov (accessed on 10 June 2021).

Devices for measuring hail include integrated sensors and time-recording hail instruments and meters. Typically, integrated sensors consist of hail pads, hail cubes, and hail wind detectors [55–60]. Hail pads are the most widely used and inexpensive method for observing hail; they can determine the occurrence of hail and estimate its size according to the degree of the depression, as well as calculate its mass using velocity and density assumptions. However, they can be used once only, and cannot function if they are blown away by the wind [55–58]. Hail cubes are similar to hail pads, and their recording time is

approximately 20% longer [55,59]. Hail wind detectors can measure the wind direction, although gusts prevent proper measurements [55,59].

Time-recording hail gauges, which are more sophisticated than integrated sensors, can record the time when the hail falls [55]. The geophone, developed by the South Dakota School of Mines and Technology, transmits electrical pulses based on the location and momentum of the impact on the plate, providing information about the size, number, and duration of hail occurrences. The Illinois State Water Survey hail gauge is mechanical and battery-operated, hence it can be installed in remote areas, although it is sensitive to strong gusts; based on ballistic pendulum theory, it measures the precise moment and duration of hail-fall for hailstones ≥ 1 cm in diameter [55,60]. Next-generation meteorological satellites offer longer observation periods, higher temporal resolution, and more observation channels, enabling them to better detect formation processes during the initial growth, peak, and decline periods of thunderstorm clouds. The early detection that they provide has improved preemptive responses to meteorological disasters and their prevention [61].

Modern radar-based hail research is being conducted against the backdrop of satellite development [2,55,62]. There are four categories of weather radar: conventional, Doppler, polarization, and parametric. Single-polarization radar, which is used in hail research, does not easily distinguish between precipitation types such as rain, snow, and hail, and generally estimates precipitation much less accurately than dual-polarization radar. Dual-polarization weather radar provides information on raindrop size and shape, and can estimate precipitation amounts via horizontal and vertical polarization [62,63]. C-band radar, which can be used to observe hail, covers a range of 120 km. S-band radar provides strongly attenuated hail location [64,65]. Despite these shortcomings, downscaling C-band radar data provides better hail forecasting estimates than other radar types [65].

4. Hail Prediction

As with all meteorological forecasting, hail-event forecasting requires observation; this presents difficulties because these events occur suddenly and sporadically in localized areas [66,67]. To reduce hail damage in aviation and to protect property such as crops, cars, and buildings, preventing significant losses, notice of hail events must be given approximately 15 min before they occur [2,68].

Historically, people predicted hail damage based on their experience [69]. For example, during the Joseon Dynasty in Korea, weather predictions were based on natural events, weather, and phenology, and on both microscale and seasonal observation of animals, plants, and natural objects [69]. Based on this phenological perspective, in which there are twenty-four solar terms in a year, hail was expected to fall 30 days before and after the summer solstice (June 21 and 22, respectively, in the lunar calendar) [69]. In associated myths, hail occurs when a cloud with the appearance of a fish scale is accompanied by wind, or when a cloud shaped like a flock of sheep lasts for three days without rain [69].

Numerical weather prediction, based on mathematical atmosphere and ocean models, has been the most widely used weather prediction method since the 1920s. The atmosphere undergoes continuous, sudden, and localized changes, and is therefore considered a 'chaos system' because small changes can alter the entire system. Because of these features of the atmosphere, hail events are difficult to forecast [66,70]. Ensemble forecasting, which has been applied globally, can improve forecasting by accounting for chaos and uncertainty [66]. Both very short-term and short-term forecasts are being used.

López et al. [66] improved forecast reliability by combining C-band radar with binary logistic regression models for an area of 50,000 km² in the northeast of the Iberian Peninsula, Spain (comprising the Central Ebro Valley, Aragon, and the province of Lleida), providing a statistical ultra-short-term hail forecasting model. They obtained a description of the atmospheric conditions, meteorological indices, and parameters on the study day, based on data obtained from a radiosonde in the center of the study area at 1200 UTC daily. The predicted hail events obtained by processing C-band radar data using TITAN software were validated using data from hail pads and a dense weather-observer network. Using

logistic regression analysis, they developed a function combining seven weather variables (total totals index, wind at 500 hPa, wind at 850 hPa, altitude of convective condensation, wet bulb zero height, dew point temperature at 850 hPa, and T^2 gust index), allowing dichotomous prediction of hailstorms based on the risk of hail-induction [66].

Similarly, Snook et al. [67] conducted ultra-short-term (warn-on-forecast) hail forecasting via numerical modeling ensemble prediction using dual-polarization radar, advanced regional prediction systems, and ensemble Kalman filter data assimilation for supercell storms in Oklahoma, USA, on 20 May 2013. By applying an advanced data assimilation system, this work introduced the possibility of storm-resolving ensembles and revealed the usefulness of high-resolution radar observation data (with 500 m horizontal grid spacing) at time scales from 0 to 90 min; hail event forecasts were validated using dual-polarization radar data [67]. Further, this work confirmed that robust predictions require the use of different convection modes at different locations [67].

Gagne et al. [68] performed short-term hail forecasting using a statistical–numerical composite model using dual-polarization radar, convection-allowing models, machine learning, and the CAPS ensemble model. Their proposed model, with a spatial resolution of 3 km and a forward prediction time of 24 h, first determines the parameters of hail occurrence and radar-estimated hailstone-size distributions, while including storm properties and global conditions in a storm prediction database. At most probability thresholds, machine learning model predictions achieved a higher critical success index, and are more reliable for predicting strong hail precipitation than other forecasting methods. This model was generated by combining two convection-allowing ensemble systems, and the results were compared with those obtained using other forecasting methods [68].

For Friuli–Venezia Giulia, a plains region in northeastern Italy, Manzato [71] applied ultra-short-term statistical forecasting using hail pad data, sounding data (sounding four times per day from the Udine-Campoformido radio-sounding station), and neural network analysis (using hail data from 1992 to 2009 from a network of approximately 360 stations). To evaluate the usefulness of fifty-two sounding-derived indices, bivariate analysis was used to relate eight indices of instability (including updraft, hailstone diameter, and updraft index) to hail-event intensity, at six-hour intervals [71].

Short-term numerical forecasting of hail events was conducted using a Weather Research and Forecasting (WRF)–HAILCAST model combined with a convection-allowing model [72]. The Advanced Research Weather and Research Forecasting (WRF) model (ARW) [32] was integrated with the HAILCAST hailstone-growth model, producing the WRF-HAILCAST model. When the WRF-HAILCAST model was run at a spatial resolution >4 km (horizontal grid spacing), it reproduced the dominant large-scale circulation and hydrometeorological fields associated with organized storm and convection systems, and generated realistic predictions at grid intervals as fine as 1 km [72].

Li et al. (2019) [48] investigated the sensitivity of hail precipitation from idealized hail to realistic environments through an ensemble of cloud-resolving simulations using meteorological research and forecasting models with initial condition perturbations derived from the ECMWF (European Centre for Medium-Range Weather Forecasting) operational ensemble [48]. As a result, it was confirmed that small-scale environmental disturbances can cause significant differences in hail precipitation rates and cloud formation processes [48]. Additionally, hail precipitation was found to be more sensitive to thermodynamic perturbations than to kinematic perturbations [48]. Initial environmental disturbances have been identified as limiting the inherent predictability of hailstones to their sensitivity [48]. More recent new ideals show simulating uncertainty from initial perturbation, not only including the meteorological perturbation but also aerosols [29,48,73–75].

5. Hail Damage and Risk Map

Hailstones cause damage to various industries. Most hail-related damage is to vegetation (90.51%) rather than property (9.49%), while it poses negligible harm to animals and people [76,77]. This is because small-scale hail is much more frequent than large-scale

hail [20,76]. Hail damages crops and trees at hailstone diameters ≥ 12.5 mm and ≥ 30 mm, respectively [51,52,76,78]. Damage to crops and trees is often initially or completely overlooked, leading to serious long-term damage [16]. Hail damages property such as cars, windows, and rooves at hailstone diameters of 50–70 mm or greater [76,79,80].

Hail typically causes substantial damage to agricultural areas. Hail causes various types of damage in different agricultural sectors (Table 2). Hail causes greater crop damage on the windward side of crop stems and branches [2]. Hail-induced crop damage can cause primary and secondary injury. Primary injury includes physical injury, such as fallen or damaged leaves, branch and soft stem breakages, stem lesions, and bark peeling. Secondary injury, including damage from fungal or bacterial infection, leads to wilting of damaged plant parts, bruising, rot, or plant death. Hail has been reported to lead to the injury, fungal infection, or death of livestock [2]. Hail-related damage to fishing grounds alters fish migration, and leads to microalgal and pathogen infection [2].

Table 2. Representative types of hail damage by agricultural sector.

Agricultural Sector	Type of Damage	References
Field crops	Stem lodging and breakage Stem bruising Fiber-quality deterioration Grain shattering Pod shedding Defoliation Secondary infection	[2,81–85]
Horticultural crops	Scars in bunches Dropping of immature fruits, berries, flower buds, or flowers Fruit cracking, lesions, and scars Stem bruising Petiole breakage and defoliation Leaf shattering	[78,86]
Vegetable crops	Lesion on fruits and leaves Fruit rotting Burning of terminal ends of leaves Stem bruising Twig breakage Leaf drying Secondary fungal infections	[2]
Fishes	Migration Damage to fishing structures Poorly understood impacts due to microalgae and pathogens	[2]
Animals	Mortality Injury Fungal infections Nest failure	[2,77]

A red pine tree forest in Hwasun, South Korea, was severely damaged by hail in 2017 (Figure 6) [15]. Cremer [81] found that, comparing trees in forested areas, pine trees (*Pinus* spp.) suffer the worst hail-related damage, both in terms of physical damage and pathogen infections (post-traumatic biological damage). In South Korea in 2017, hail caused significant damage to pine trees (*Pinus densiflora* and *Pinus rigida*), with brown discol-

oration occurring 7–10 days after the hail event; cypress (*Chameacypais obtusa*) suffered stem scarring, soil loss and some leaf loss, although the injuries were not life-threatening [15]. Likewise, cedar (*Cryptomeria* spp.) and chestnut (*Castanea crenata*) trees suffered minor damage, and hardwood trees suffered some branch breakage and leaf fall but no serious damage [15]. In October 1994, hail caused severe damage to mangrove forests in Port Curtis, Australia [87]. Like the hail damage in South Korea, this hail stripped leaves from plants, punched holes through the leaves, bruised the bark, and removed divots from the bark, leading to branch and plant death [87]. Of the three common mangrove species in these forests (*Rhizophora stylosa*, *Ceriops tagal*, and *Avicennia marina*), *C. tagal* was most vulnerable to the effects of hail and showed relatively higher mortality [87]. During the 2017 spring nesting season in north-central Pennsylvania, localized precipitation of hailstones of approximately 2.5 cm in diameter caused 89% nest failure for the golden-winged warbler (*Vermivora chrysoptera*), and 7 of the 8 failed nests contained broken eggs; this nest loss was attributed to the loss of saplings and canopy trees [18].



Figure 6. Photograph of a damaged Korean red pine (*Pinus densiflora*) forest in Hwasun (South Korea), showing ‘severe’-grade hail damage. Insets: damaged branches and twigs. Adapted from [15].

Hail also causes damage to property in densely populated areas as well as agricultural and forested areas. Hail damage to buildings is more highly correlated with maximum hailstone size than with the number of hail strikes per unit surface area [88]. According to Munich Re [89], a hailstone diameter of 19 mm is the minimum threshold for serious property damage. For hailstones >50 mm in diameter, Charlton et al. [90] found that residential buildings with tiled roofs experienced worse hail damage than commercial buildings with graveled tar roofs. In terms of claim severity for hail-induced roof damage, Brown et al. [50] found that the most claims were for wood rooves (9.6%) and metal rooves (9.2%), while tile rooves (2.9%) accounted for the fewest claims (Figure 7). Similarly, buildings constructed of fiber, wood, and aluminum have a higher potential for hail damage than those constructed of brick [91].

The amount of energy transmitted by hail is related to the potential damage to building materials, and can be used to estimate the hail damage potential index for roofing and glazing in the construction industry (Figure 8) [41,92–94]. Rhodes [94] found that various roofing materials were damaged by hail, and Morrison [93] investigated the relationship between hail size and damage to building material. Hail with a diameter of 19.05 mm damaged painted wood and aluminum materials (vents and drains), and at 25.4 mm it could break a single glass window. Based on laboratory impact testing, hail of 25.4 mm in

diameter damaged asphalt roofs and could break a vehicle’s windshield; and at 31.75 mm, it could damage vehicle surfaces. Hail of 50.8 mm in diameter could damage concrete tiles [93]. Notably, the reported size-thresholds for hail damage based on field data tend to be smaller than those based on laboratory testing [50,93,95].

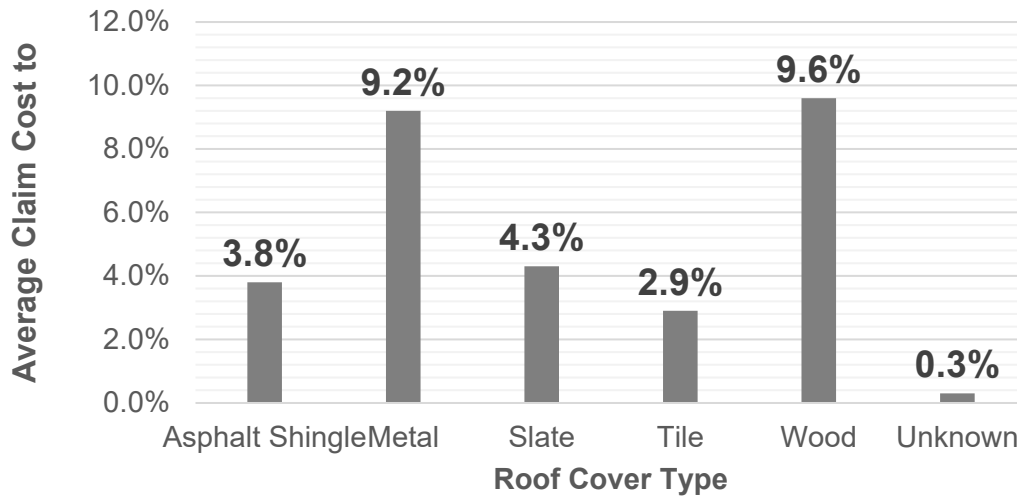


Figure 7. Average roof-claim severity normalized by coverage limit (ratio of costs to insured value), by roofing type. Data from [50].

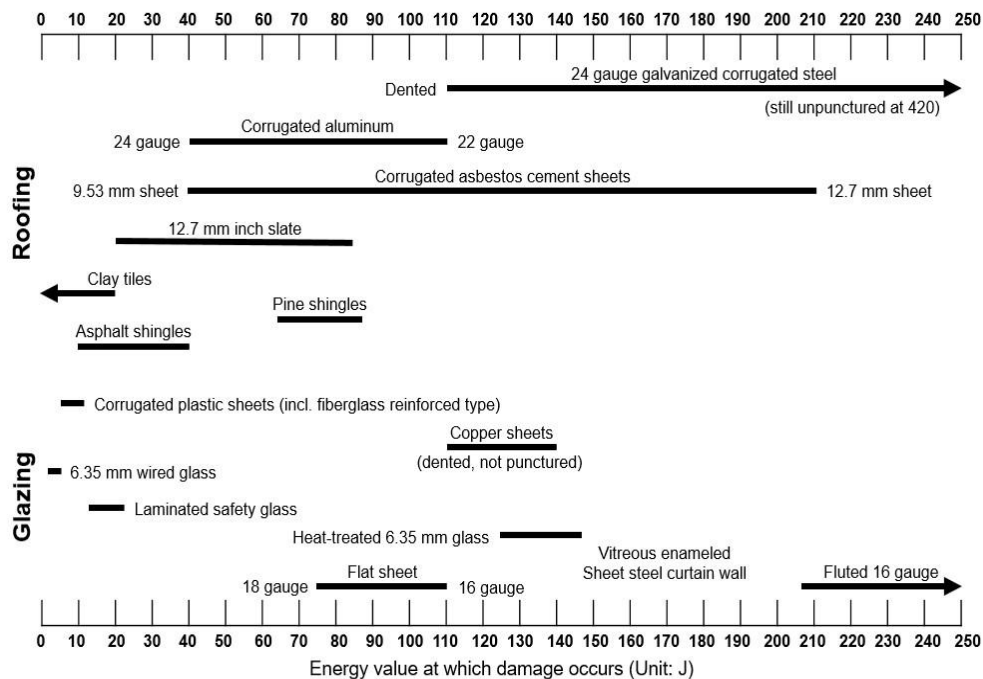


Figure 8. Relative sensitivity of various building materials to energy levels imparted by hail. Data from [41].

Hail damages photovoltaic panels by damaging the cell surface and causing invisible microcracks that impair electricity generation [94,96]. Mathiak et al. [97] found that at 6 cm hail diameter, 42% of module cells exhibited visible damage; at 4 cm, 3% of module cells exhibited visible damage, and 90% of microcracks were star-shaped [97]. Moore and Wilson [98] conducted experiments on the effects of hail on photovoltaic panels, finding that the degree of hail impact differed depending on the surface layer of the panel: silicon

potting provided the weakest protection against hail, while annealed glass and tempered glass provided the strongest protection [98].

The global distribution of hail precipitation has been studied to investigate how best to estimate hail frequency [19,20,99–102]. Prein and Holland [19] estimated and cross-validated the frequency of large-hailstone precipitation using data from large-hailstone events (diameter >2.5 cm) and daily ERA-interim (a reanalysis of the global atmosphere covering the data-rich period since 1989) reanalysis data for the continental USA from 1979 to 2015. Using this data, Allen et al. [20] confirmed that hail occurs mainly in the mid-latitude continental regions, decreases in frequency toward the polar regions and the equator. Globally, hail occurs frequently in the USA, Australia, China, India, and the Great Plains of Central Europe and Central Asia [19,20,41].

Figure 9 illustrates the average probability of heavy hail (>2.5 cm in diameter) globally from 1979 to 2015. Although hailstone size plays the biggest role in hail-induced human casualties, the risk of casualty increases with the population density [19,76].

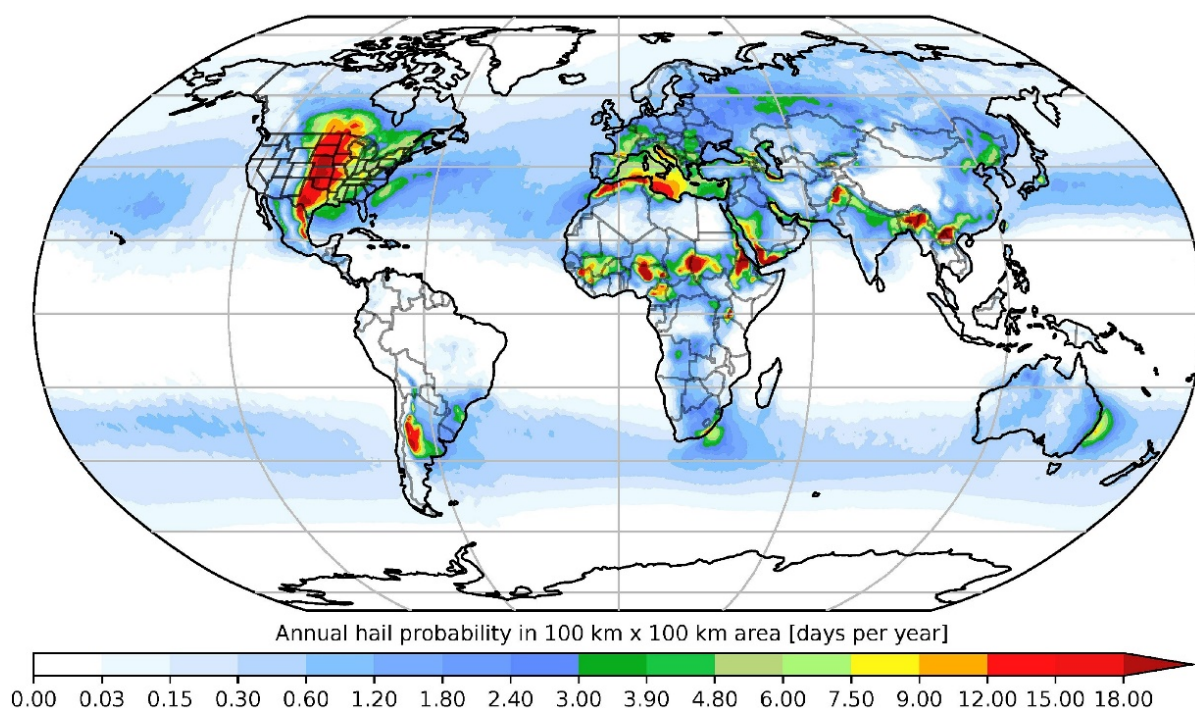


Figure 9. Worldwide average annualized probability of heavy hail, normalized to an area of 100×100 km, from 1979 to 2015. Adapted from [19].

Figure 10 illustrates the locations of hail-monitoring stations and the distribution of hailstone diameters in China from 1980 to 2015 [103]. China covers a large territory, and therefore exhibits varied topography and associated meteorological phenomena. In China, hailstone size varies depending on the terrain, with average diameters of 10 mm on the highlands (above 2000 m) and of 20 mm in the foothills (at 500–2000 m) and plains (below 500 m). In China, hailstone diameter has continuously decreased since 1990, and hail frequency decreased significantly in the 1980s and 1990s [103].

Reports of hail-induced injury to humans are significantly less frequent than those of damage to crops and buildings, and the severity of the injury is not often mentioned [57]. Figure 11 shows the numbers and locations of hail-related human injuries in Europe and the USA [19,76]. Figure 12a illustrates the magnitudes reported to the European Severe Weather Database up to September 2015 [17]. According to Punge and Kunz [17] and Púčík et al. [76], a high incidence of very large-diameter hail (i.e., in southern Germany, northern Italy, the Balkans, southern Russia, and the midwestern USA) tends to coincide with a high incidence of severe injuries.

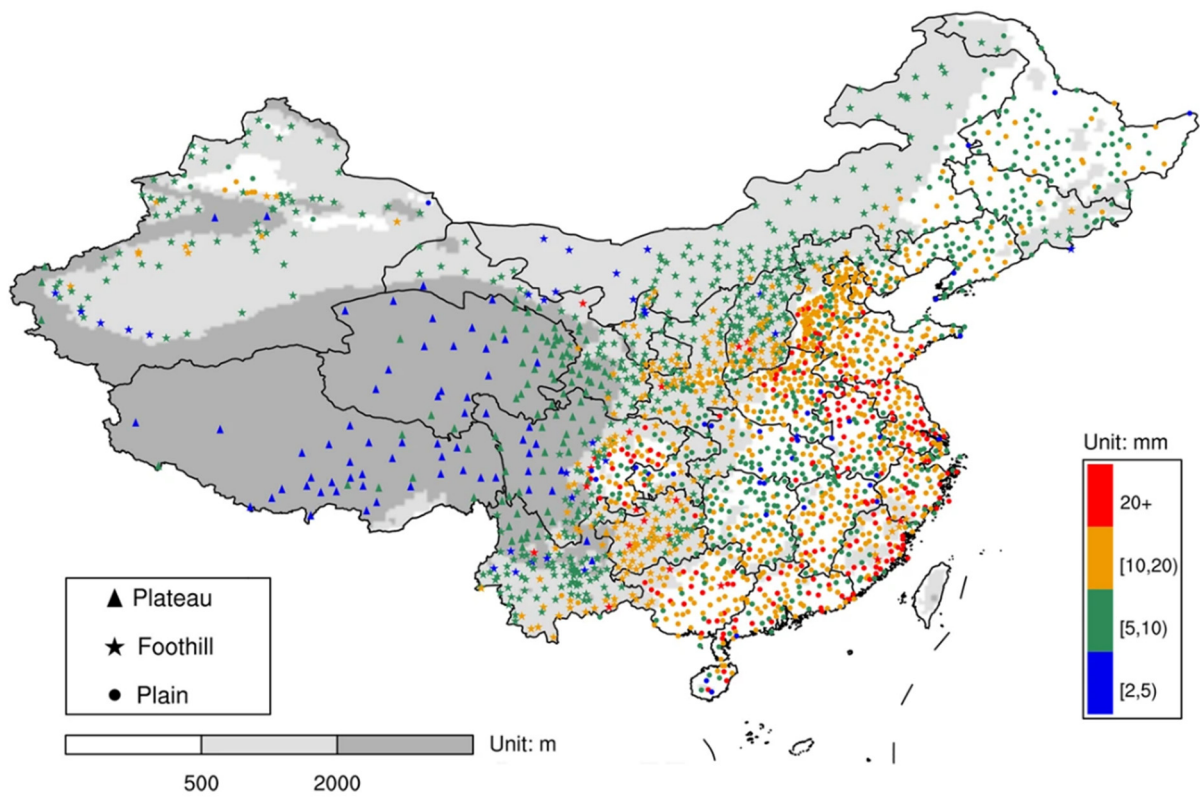


Figure 10. Distribution of hailstone diameters, and location of 2254 hail-monitoring stations, between 1980 and 2015. Adapted from [103].

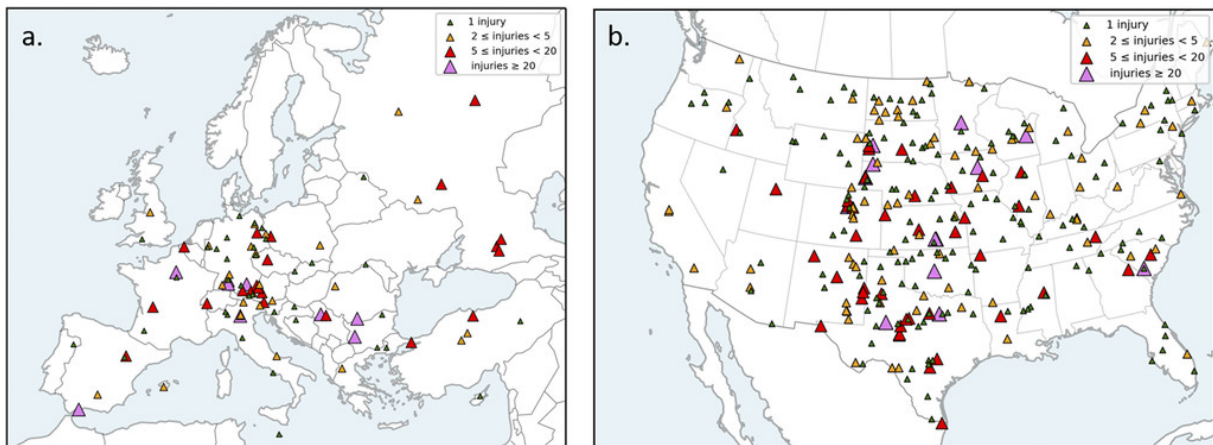
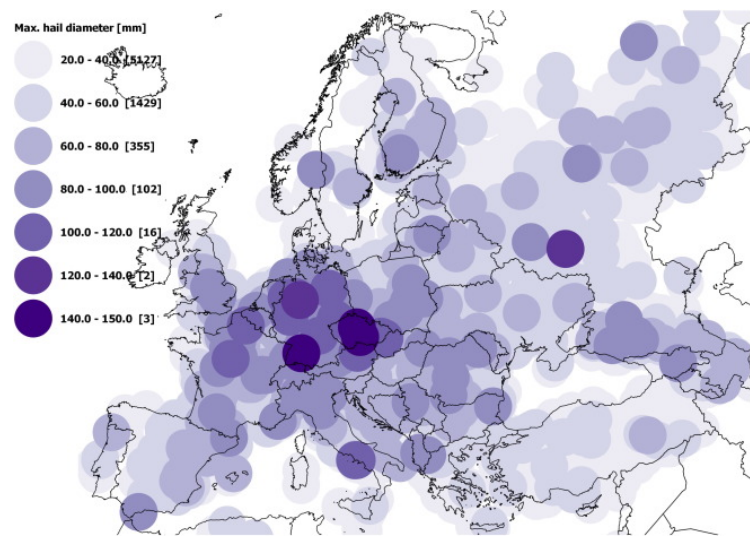
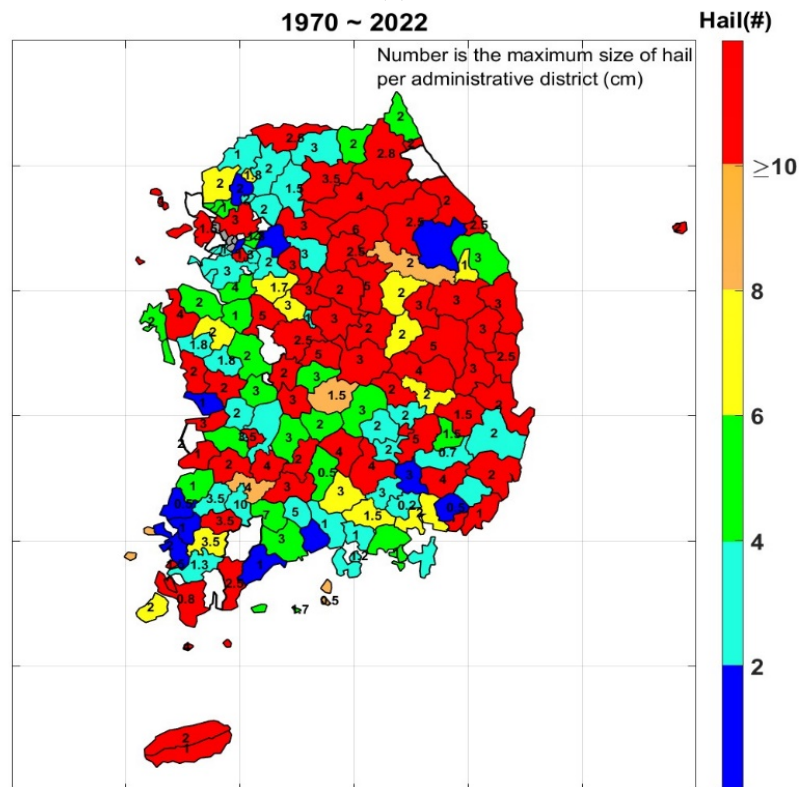


Figure 11. Hailstone-related injuries in (a) Europe and the (b) USA. Adapted from [76].



(a)



(b)

Figure 12. (a) Maximum hailstone diameters (mm) reported to the European Severe Weather Database in defined locations up to September 2015. Adapted from [17]. (b) Hail risk map based on the KMA observation and Newspaper information in South Korea from 1970 to 2022. The numbers in each administrative district reflect the maximum hailstone size and the color shows hail frequency. Adapted from [104].

In Central Europe, hail occurs frequently due to the influence of the continental region, presenting high risks [17]. Due to its proximity to the Atlantic Ocean, Western Europe is more meteorologically stable than Central Europe, and is characterized by year-round formation of small hailstones [17]. Because of its hot and humid climate, parts of Southern Europe have some of the highest hail frequencies in Europe. Northern Europe is

predominantly colder than the rest of Europe; its proximity to the North Atlantic suppresses strong convective activity, resulting in the formation of small hailstones year-round [17,36].

The deadliest hail event occurred on July 12, 1984, in Munich (Germany), injuring 400 people (Table 3), followed by an event in Fort Worth (USA) that injured 109 people. Although the size of the hailstones falling in Reutlingen (Germany) in 2013 was not officially recorded, they were reported to be as large as ostrich eggs [76]. Similarly, for a hail even in Romania (June 1997) that injured 60 people and killed four people, the size of the hailstones was not published, although newspapers reported that they were as large as ostrich eggs [76,105]. On July 23, 1988, hail in France caused secondary damage to a building, causing the roof to collapse under the weight of the hail, resulting in many casualties [76].

Table 3. Hail events ranked by the number of human casualties in Europe and the USA.

Date	Country	Location	Number of Casualties
12 July 1984	Germany	Munich	400
5 May 1995	USA	Fort Worth	109
28 July 2013	Germany	Reutlingen	74
20 June 1997	Romania	Apele Vii	60
8 July 2014	Bulgaria	Sofia	40
23 July 1988	France	Torcy	33
21 September 2007	Serbia	Indija	30
4 August 2002	Spain	Marbella	30

Adapted from Púčik et al. [76].

In South Korea, A hail information service system was developed to understand the temporal and spatial distribution of hail occurrence [104]. As part of the system, a hail observation database was established that integrated the observation data from Korea Meteorological Administration (KMA) with the information from newspaper reports. A hail risk map was produced based on this database (Figure 12b). The risk map presented the nationwide distribution and characteristics of hail showers from 1970 to 2018, and the northeastern region of South Korea was found to be relatively dangerous. By integrating multidisciplinary data, the temporal and spatial gap in hail data could be supplemented. The hail risk map produced in their study is used for the selection of suitable crops and growth management strategies under the changing climate conditions.

6. Hail Damage Compensation Systems

Hail causes various types of damage affecting humans, and is therefore one of the few types of weather events that is covered by insurance in many parts of the world [106–108]. For instance, in North America, there are many agricultural insurance options, covering aspects such as farm revenue and yield, and European insurers provide farmers with the most necessary coverage [108,109]. Agricultural insurance related to meteorological disasters such as hail is compulsory in Switzerland, the Republic of Azerbaijan, and the USA [108,110,111].

In the European Union, the Common Agricultural Policy considers risks when providing farmers with meteorological disaster insurance [112]. In Switzerland, hail insurance also covers risks such as flood and storm damage; although there is no government subsidy, insurance premiums were subsidized at the canton level at 0.03% in 2009 [108,112]. In Switzerland, the hail insurance participate rate gradually decreased from about 70% in 1990 to 56% in 2002, then increased slightly in 2004, and has since tended to decrease [112]. Finger and Lehmann [112] found that the people who took out hail-related insurance in

Switzerland were relatively older, more educated, and more likely to be from farms in areas where hail occurred frequently.

In the Republic of Azerbaijan, laws related to agricultural insurance were adopted on 27 June 2019, and the Central Agricultural Insurance System Research Institute was established. Since 1 January 2020, Azerbaijan has continuously acted to formalize new types of agricultural insurance, tailoring insurance coverage to the crops and their associated risks; although the weather conditions guaranteed for each crop differ slightly, hail-related compensation is commonly included (Table 4) [113].

Table 4. Guaranteed Insurance and weather risks covered by crop insurance in Azerbaijan.

Crop Name	Weather Risks Covered by Insurance	Rationale for These Options
Wheat	Hail, Fire, Storm, Hurricane, Landslide, Earthquake	Improves food security
Barley		
Corn		
Potato		
Sugar beet		
Orange	Hail, Fire, Storm, Hurricane, Landslide, Earthquake, Loss of quality due to hail	Affected by import substitution policy
Lemon		
Tangerine		
Tea	Hail, Fire, Storm, Hurricane, Landslide, Earthquake	
Tobacco		
Rice		
Grapes	Hail, Fire, Storm, Hurricane, Landslide, Earthquake, Loss of quality due to hail	Strengthens export potential
Hazel		
Cotton		

Adapted from Khudiyev and Dadashov [113].

The USA provides national support for agricultural insurance, helping to reduce insurance costs for farmers primarily via subsidized premium payments. According to the Agricultural Protection Act of 2000 and the Food, Environment, and Energy Act of 2008, US agricultural programs include crop insurance, profit insurance management, crop insurance index, insurance income, insurance income schemes, and cultural cultivation insurance income to systematically manage crops [114]. Federal crop insurance is available only from private insurance companies; publicly operated management agencies oversee the activities of these companies and provide quality control inspection services [114,115].

7. Hail Disaster Management

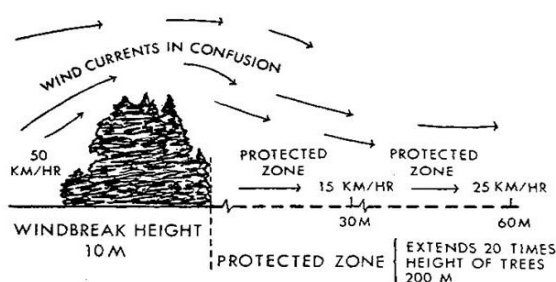
Although hail observation and forecasting are used to reduce hail damage, disaster prevention tools are required to preemptively mitigate hail damage. Both physical and chemical methods are currently used [2,42,116–118]. Anti-hail nets and shelter belts (wind-breaks) are proposed as physical methods for hail disaster prevention (Figure 13) [2,77,119]. Anti-hail nets (protective screens) are a standard and effective anti-hail disaster prevention tool [3,119,120]. They have relatively low installation costs and high durability, offering continual crop protection, but are ineffective against large hailstones (>2.5 cm diameter) [2]. They reduce light transmittance and affect the microclimate of the orchard, by reducing the maximum temperature, increasing the minimum temperature, and reducing wind speed [120–122]. Meszaros [119] found that these microclimatic changes reduced the average yield per tree and negatively affected total growth, while improving Nitrogen and

Phosphorous absorption and split into leaves and fruits, and improving accumulation of the leaf trace-elements iron, zinc, and manganese [86]. According to Lee et al. [5], anti-hail nets are typically lowered and erected using a human-operated motorized system, but are folded and unfolded manually; they proposed an automated system providing faster net-unfolding, and are developing hail-detection sensors for anti-hail netting.

Hail, and hail damage, is often accompanied by particularly strong winds. Shelterbelts are used for hail-disaster prevention in orchards and fields because they protect against strong winds [119,123], by directly blocking the wind or redirecting the airflow [2,121,124]. The damage to crop plants is greater on the windward side of the plant [2,82–86,125].



(a) Orchard anti-hail netting on concrete structure in northern Italy



(b) Functioning of a windbreak (shelterbelts)

Figure 13. Hail-damage prevention measures. Adapted from: (a) [122]; (b) [124].

Anti-hail cannons are used to create shock waves that melt the ice particles in the clouds, physically impeding hail formation and growth (Figure 14) [2,126]. First developed in 1896 by Albert Stiger, an Austrian wine farmer, they originally used gunpowder to produce shock waves from a cone-shaped vertical muzzle (Figure 14a) [2,42]. Their usage increased massively initially but had declined by the end of 1906. A new anti-hail cannon model (Figure 14b), developed in 1972 by Corballan, a French company, was widely used in Spain, Canada, and Belgium [42,116]. Contemporary anti-hail cannons, which direct blasts of sound at high volumes (≥ 120 dB) upward using butane gas or acetylene, are actively used in agricultural areas in Italy, France, Austria, the Netherlands, the USA, Australia, New Zealand, and China [2,42]. As the shock waves do not affect hail that has already formed, anti-hail cannons must be activated 20 min before the formation of hail clouds, thus improving their effectiveness [2]. As such, the use of hail-tracking devices, such as doppler radar, is recommended to ensure the effectiveness of anti-hail cannons [2,42,127].

A schematic diagram depicting the cloud seeding process is shown in Figure 15 and details are as follows. Cloud-seeding, a chemical hail-disaster prevention method [125] developed in the 1940s, reduces of cumulonimbus cloud size or reduces and decomposes hailstones using chemical substances, such as silver iodide (AgI), potassium iodide (KI), sodium iodide (NaI), dry ice, or liquid propane [2,36,128–130]. These chemicals disperse cumulonimbus clouds via microphysical changes [87]. For instance, when using an AgI–NaI acetone solution, providing the acetone without solid fuel or combustible gas causes it to generate a vortex at $750\text{ }^{\circ}\text{C}$, completely vaporizing the silver iodide, which is then unable to break down the hail [36]. Although the effectiveness of cloud seeding remains controversial, Ćurić et al. [127] found that when used in the early stages of cloud development, it reduced hail by 6.74% and increased rainfall by 8.43%, thereby confirming that silver iodide contributes to hailstone reduction.

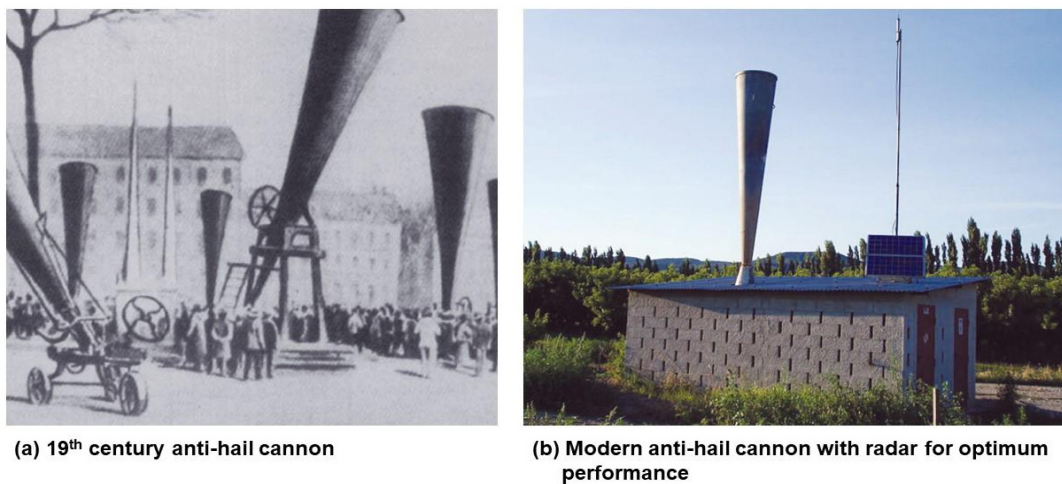


Figure 14. Examples of past and present anti-hail cannons. Adapted from [122].

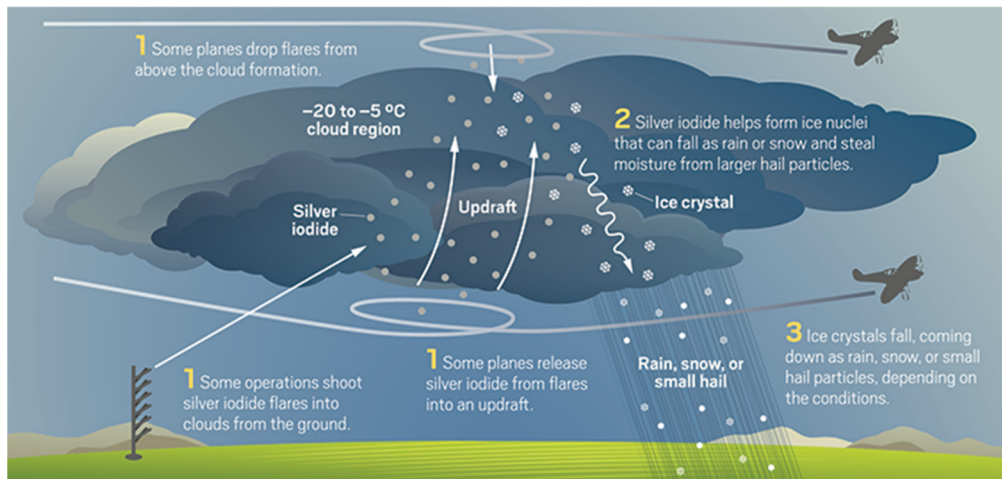


Figure 15. Schematic diagram depicting the cloud seeding process. Adapted from [125].

The chemical substances used to reduce hail precipitation are commonly dispersed using anti-hail rockets or via aircraft seeding [2,36,43,131] (Figure 16). Anti-hail rockets disrupt the growth phase of hailstorms [87].

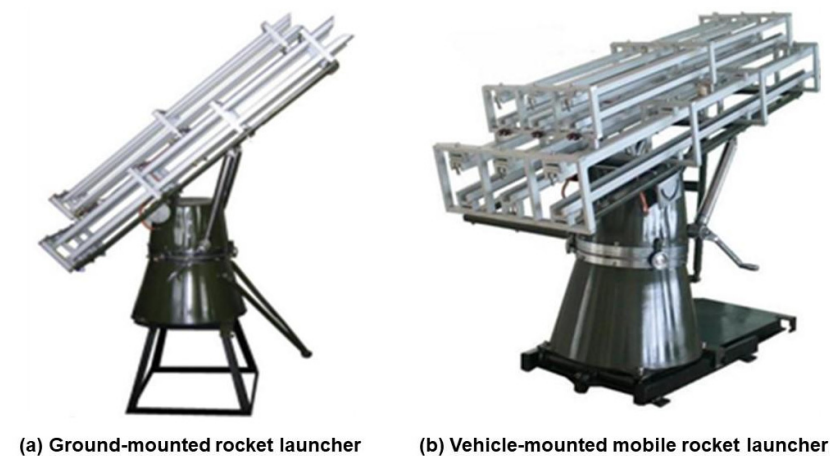


Figure 16. Examples of anti-hail rocket launcher systems. Adapted from [1].

After the hailstorm starts, a chemically equipped rocket is launched; this reduces hail precipitation, and the clouds disappear [1,42,127,132]. Anti-hail rockets can fly up to 10,000 m, and are suitable for protecting complex areas including large-scale vine farms and fruit orchards. They inject chemicals into the clouds, rapidly reducing hail formation; however, suitable launch points must be located on farms and in protected areas, and launches must not obstruct air traffic [17]. Anti-hail rockets are widely used in Russia, Italy, China, Kenya, and the Balkans [42,133,134].

Aircraft seeding, via the cloud-base or cloud-top approach, is commonly used in areas where anti-hail rocket infrastructure is unavailable or launching is not possible; it has been used successfully in Canada, the USA, Argentina, China, and Germany, effectively removing up to 40% of cloud-residing hail [35,135]. The cloud-base approach sprays AgI as the plane passes beneath the cloud; the cloud-top approach more effectively and directly removes ice crystals by spraying it over the top of cloud [135]. Aircraft seeding for hail suppression is still being critically assessed, due to its high costs and the difficulty and operational risks associated with flying in complex storm systems and during the night [36,135].

The Association Nationale d'Etude et de Lutte contre les Fléaux Atmosphériques (Association to Suppress Atmospheric Plagues; ANELFA) network for hail research and prevention in France conducts hail prevention (Figure 17). When the ANELFA network was initially formed, it comprised only a few generators along the Pyrenees and the south Atlantic coast of France, but by 1984 it had expanded to provide hail protection to an area of 55,000 km² [36]. It has since expanded to 70,000 km², including the French wine-growing region as of 2015 [36].

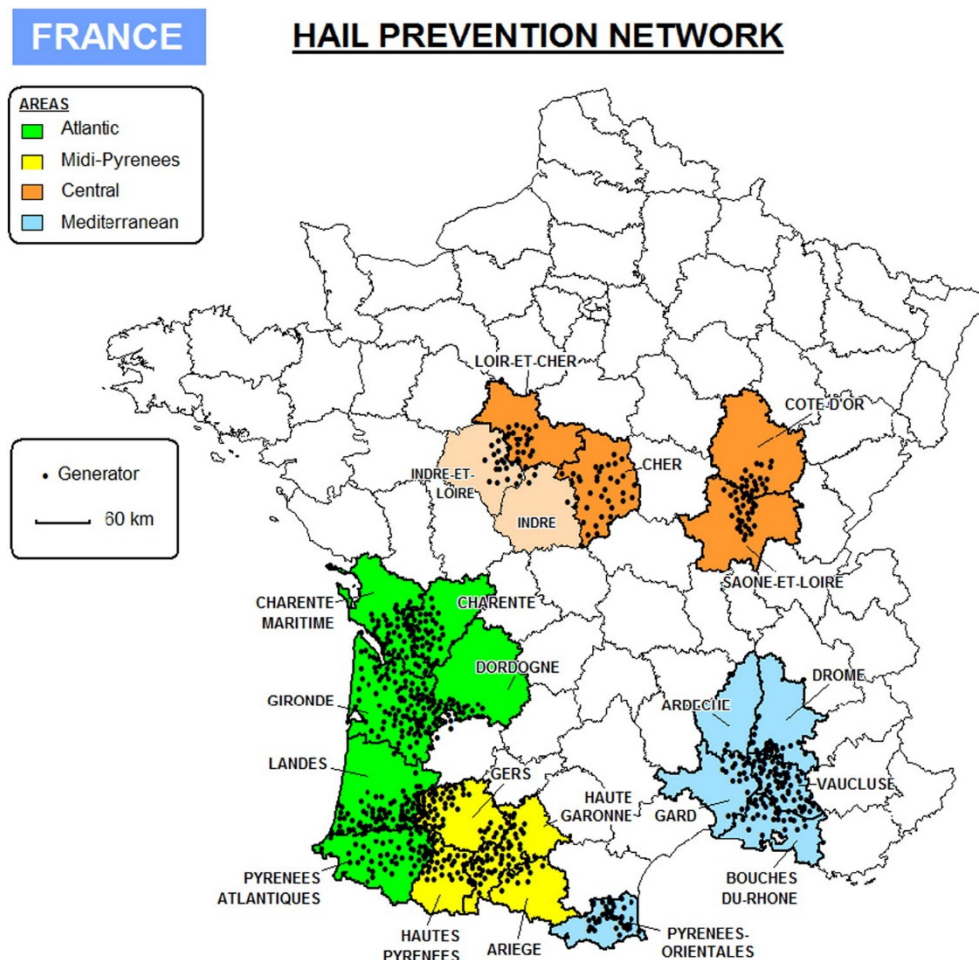


Figure 17. Distribution of ANELFA network generators in France in 2015. Adpated from [36].

Yuter and Houze [134] proposed a model that accounts for stratified transition in storm convection by linking vertical mass transport and mass divergence. In this model, vertical mass transport occurs widely during precipitation, and relatively low intensity upward velocity is critical to mass transport; in a few places, strong vertical motion disperses all of the hail particles deep within the storm cloud. In the same paper [134], those authors proposed a conceptual convection model based on bubbles, to explain the transition from convection to stratification: in this model, a bubble of buoyant air formed at a low altitude is slowed by the change in the amount of air it contains as it ascends, causing it to stop at middle and upper altitudes and to spread out sideways. An ensemble model combining these two models has been proposed [36]. This proposed multicellular cumulonimbus ensemble model (Figure 18) uses radar data and numerical simulations to ensure that cloud seeding proceeds correctly, for simulated thunderstorms in Florida [36,134]. The model of Yuter and Houze [134] has been applied elsewhere in the world to effectively reduce thunderstorms.

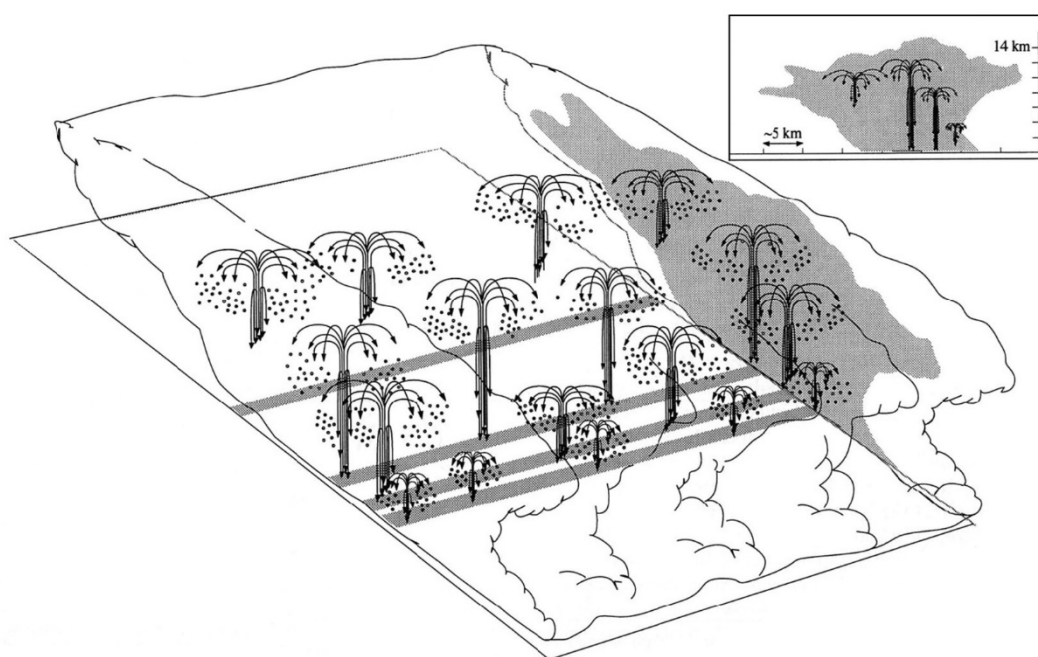


Figure 18. Conceptual model of an ensemble of hail particle fountains in a multicellular storm in perspective view. Adapted from [134].

8. Summary and Concluding Remarks

With climate change, hail-event frequency is changing differently on different continents. In East Asia, hail precipitation frequency and hailstone size has decreased, and hail precipitation frequency has decreased in Australia; in Europe, hail precipitation intensity has increased, and the environment is becoming more suitable for hail growth; and in North America, although clear overall environmental changes could not be observed, conditions for large hailstone growth have developed in certain areas [6]. In all regions, however, hail events are localized and sudden, causing damage to agriculture, industry, and houses. Globally, the frequency of hail events has changed, and hail-related damage has changed quite proportionally.

The magnitude and characteristics of hail-related damage can be classified based on hailstone size [51–53], relying primarily on NOAA classifications. Due to severe climate change, entirely new approaches are necessary to study the microphysical aspects of hail growth [6]. In future, studies of the microphysical aspects of hail should be combined with modeling research to elucidate how climate change is affecting hail growth. Hailstones of all sizes can cause primary and secondary hail damage. It is necessary to study hail-related damage attributable to microorganisms to fully understand hail-related damage.

Furthermore, although the basic mechanisms of hail growth have been elucidated, in terms of the atmospheric environment and materials [17,20,22–25,28,45–47], the thermodynamical and geophysical conditions leading to hail formation now occur more frequently, and further research is needed. While anti-hail nets, which are relatively inexpensive and easy to access, help to prevent hail-related damage in agricultural areas, they cause microclimate changes. These changes, and their impacts on crops, require further research in agricultural engineering and biogeochemical fields.

The sudden and localized nature of hail events makes it difficult to observe and forecast such events. The duration of hail events can be determined at ground level using time-recording instruments with integrated hail sensors. Hail events can also be observed via remote-sensing radar: dual-polarization radar can measure reflection, crossphase effects arising from crossphase modulation, differential reflection, and non-permeability [66]. A numerical model based on crossphase radar data has been applied along with machine learning for short-term hail event forecasting [66]. As the media system develops, newspaper articles database and SNS text information can be used as auxiliary data to supplement insufficient hail observation information, and need to be upgraded.

Much research effort is being put into studying hail-disaster prevention via physical and chemical methods. This review, and the ongoing research on hail-related damage, reveals the progress that has been made in developing hail-forecasting science and technology, and will help nations and people to wisely manage and reduce hail-related damage.

Author Contributions: Conceptualization, S.-J.L.; methodology, M.H.K. and S.-J.L.; software, M.H.K. and J.L.; validation, J.L. and S.-J.L.; formal analysis, M.H.K., J.L. and S.-J.L.; investigation, M.H.K., J.L. and S.-J.L.; resources, S.-J.L.; data curation, M.H.K.; writing—original draft preparation, M.H.K., J.L. and S.-J.L.; writing—review and editing, M.H.K. and S.-J.L.; visualization, M.H.K., J.L. and S.-J.L.; supervision, S.-J.L.; project administration, S.-J.L.; funding acquisition, S.-J.L. All authors have read and agreed to the published version of the manuscript.

Funding: This study was funded by Rural Development Administration (PJ014879052022) in Republic of Korea.

Institutional Review Board Statement: Not applicable.

Informed Consent Statement: Not applicable.

Data Availability Statement: Data available in a publicly accessible repository. The data presented in Figure 2 and Figure 3 can be obtained with optional login information on Google Scholar at <https://scholar.google.com> (accessed on 29 September 2023) and the Scopus search engine at <https://www.elsevier.com/solutions/scopus> (accessed on 29 September 2023).

Acknowledgments: This study was carried out with the support of Cooperative Research Program for Agriculture Science and Technology Development (Project No. PJ014879052022), Rural Development Administration, Republic of Korea. The authors are grateful to Kyo-Moon Shim and Jaecheol Nam for their support and review.

Conflicts of Interest: The authors declare no conflict of interest. Author Jaeyong Lee is an employee of Geosystem Research Corporation. The paper reflects the views of the scientists, and not the Corporation.

References

1. Dong, W.; Ma, S.; Rong, B. A New Design of Rain and Hail Prevention Rocket Launch System. *Instrum. Equip.* **2019**, *7*, 1–7. Available online: <https://www.hanspub.org/journal/PaperInformation.aspx?paperID=28624> (accessed on 31 December 2021).
2. Bal, S.K.; Saha, S.; Fand, B.B.; Singh, N.P.; Rane, J.; Minhas, P.S. *Hailstorms: Causes, Damage and Post-hail Management in Agriculture. Technical Bulletin No. 5*; National Institute of Abiotic Stress Management: Pune, India, 2014.
3. Botzen, W.; Bouwer, L.; van den Bergh, J. Climate change and hailstorm damage: Empirical evidence and implications for agriculture and insurance. *Resour. Energy Econ.* **2010**, *32*, 341–362. [CrossRef]
4. Brooks, H. Severe thunderstorms and climate change. *Atmos. Res.* **2013**, *123*, 129–138. [CrossRef]
5. Lee, S.; Kim, W.J.; Kang, I.K. An implementation of an unmanned automation system for protection of crops from hail damage. *J. Korean Inst. Inf. Technol.* **2010**, *8*, 7–14. (In Korean)
6. Raupach, T.H.; Martius, O.; Allen, J.T.; Kunz, M.; Lasher-Trapp, S.; Mohr, S.; Rasmussen, K.L.; Trapp, R.J.; Zhang, Q. The effects of climate change on hailstorms. *Nat. Rev. Earth Environ.* **2021**, *2*, 213–226. [CrossRef]

7. Taszarek, M.; Allen, J.T.; Púčík, T.; Hoogewind, K.A.; Brooks, H.E. Severe convective storms across Europe and the United States. Part II: ERA5 environments associated with lightning, large hail, severe wind, and tornadoes. *J. Clim.* **2020**, *33*, 10263–10286. [[CrossRef](#)]
8. Wouters, L.; Boon, M.; van Putten, D.; Veen, B.V.; Koks, E.; de Moel, H. *A Hail Climatology of the Netherlands*; IVM Institute for Environmental Studies: Amsterdam, The Netherlands, 2019; 35p.
9. Trapp, R.J.; Hoogewind, K.A.; Lasher-Trapp, S. Future Changes in Hail Occurrence in the United States Determined through Convection-Permitting Dynamical Downscaling. *J. Clim.* **2019**, *32*, 5493–5509. [[CrossRef](#)]
10. Anderson, G.D. The first weather satellite picture. *Weather* **2010**, *65*, 87. [[CrossRef](#)]
11. Chen, H.; Lim, S.; Chandrasekar, V.; Jang, B.J. Urban hydrological applications of dual-polarization X-band radar: Case study in Korea. *J. Hydrol. Eng.* **2017**, *22*, E5016001. [[CrossRef](#)]
12. Knight, C.A.; Knight, N.C. Hailstorms. In *Severe Convective Storms*; American Meteorological Society: Boston, MA, USA, 2001; pp. 223–254.
13. Coffey, B.E.; Parker, M.D.; Thompson, R.L.; Smith, B.T.; Jewell, R.E. Using near-ground storm relative helicity in supercell tornado forecasting. *Wea. Forecast.* **2019**, *34*, 1417–1435. [[CrossRef](#)]
14. Choi, D. Army Helicopters Damaged after Heavy Winds, Rain and Hail Pelt Base in South Korea. Stars and Stripes. 2021. Available online: <https://www.stripes.com/branches/army/2021-10-04/damaged-helicopters-us-army-south-korea-storm-3120234.html> (accessed on 31 December 2021).
15. Lim, J.H.; Kim, E.; Lee, B.; Kim, S.; Jang, K. An analysis of the hail damages to Korean forests in 2017 by meteorology, species and topography. *Korean J. Agric. For. Meteorol.* **2017**, *19*, 280–292, (In Korean with English Abstract).
16. Field, C.B.; Barros, V.R.; Dokken, D.J.; Mach, K.J.; Mastrandrea, M.D.; Bilir, T.E.; Chatterjee, M.; Ebi, K.L.; Estrada, Y.O.; Genova, R.C. *Climate Change 2014: Impacts, Adaptation and Vulnerability*; Intergovernmental Panel on Climate Change: Geneva, Switzerland, 2014.
17. Punge, H.; Kunz, M. Hail observations and hailstorm characteristics in Europe: A review. *Atmos. Res.* **2016**, *176–177*, 159–184. [[CrossRef](#)]
18. Eccel, E.; Cau, P.; Riemann-Campe, K.; Biasioli, F. Quantitative hail monitoring in an alpine area: 35-year climatology and links with atmospheric variables. *Int. J. Climatol.* **2012**, *32*, 503–517. [[CrossRef](#)]
19. Prein, A.F.; Holland, G.J. Global estimates of damaging hail hazard. *Weather Clim. Extrem.* **2018**, *22*, 10–23. [[CrossRef](#)]
20. Rana, V.S.; Sharma, S.; Rana, N.; Sharma, U.; Patiyal, V.; Banita; Prasad, H. Management of hailstorms under a changing climate in agriculture: A review. *Environ. Chem. Lett.* **2022**, *20*, 3971–3991. [[CrossRef](#)]
21. Allen, J.T.; Giammanco, I.M.; Kumjian, M.R.; Punge, H.J.; Zhang, Q.; Groenemeijer, P.; Kunz, M.; Ortega, K. Understanding Hail in the Earth System. *Rev. Geophys.* **2020**, *58*, e2019RG000665. [[CrossRef](#)]
22. Houze, R.A., Jr. *Cloud Dynamics*; Academic Press: Cambridge, MA, USA, 2014.
23. Pruppacher, H.R.; Klett, J.D. *Microphysics of Clouds and Precipitation: Reprinted 1980*; Springer Science & Business Media: Berlin/Heidelberg, Germany, 2012.
24. American Meteorological Society. Hail. Glossary of Meteorology. 2017. Available online: <http://glossary.ametsoc.org/wiki/hail> (accessed on 10 June 2021).
25. Knight, C.A.; Ehhalt, D.H.; Roper, N.; Knight, N.C. Radial and tangential variation of deuterium in hailstones. *J. Atmos. Sci.* **1975**, *32*, 1990–2000. [[CrossRef](#)]
26. Nelson, S.P. The influence of storm flow structure on hail growth. *J. Atmos. Sci.* **1983**, *40*, 1965–1983. [[CrossRef](#)]
27. Ziegler, C.L.; Ray, P.S.; Knight, N.C. Hail growth in an Oklahoma multicell storm. *J. Atmos. Sci.* **1983**, *40*, 1768–1791. [[CrossRef](#)]
28. Dennis, E.J.; Kumjian, M.R. The impact of vertical wind shear on hail growth in simulated supercells. *J. Atmos. Sci.* **2017**, *74*, 641–663. [[CrossRef](#)]
29. Li, X.; Zhang, Q.; Zhou, L.; An, Y. Chemical composition of a hailstone: Evidence for tracking hailstone trajectory in deep convection. *Sci. Bull.* **2020**, *65*, 1337–1339. [[CrossRef](#)] [[PubMed](#)]
30. Fan, J.; Leung, L.R.; Rosenfeld, D.; Chen, Q.; Li, Z.; Zhang, J.; Yan, H. Microphysical effects determine macrophysical response for aerosol impacts on deep convective clouds. *Proc. Natl. Acad. Sci. USA* **2013**, *110*, E4581–E4590. [[CrossRef](#)] [[PubMed](#)]
31. Lamb, D.; Verlinde, J. *Physics and Chemistry of Clouds*; Cambridge University Press: New York, NY, USA, 2011.
32. Friedrich, K.; Wallace, R.; Meier, B.; Rydell, N.; Deierling, W.; Kalina, E.; Motta, B.; Schlatter, P.; Schlatter, T.; Doesken, N. CHAT: The Colorado Hail Accumulation from Thunderstorms Project. *Bull. Am. Meteorol. Soc.* **2019**, *100*, 459–471. [[CrossRef](#)]
33. Feldmann, M.; Hering, A.; Gabella, M.; Berne, A. Hailstorms and rainstorms versus supercells—A regional analysis of convective storm types in the Alpine region. *NPJ Clim. Atmos. Sci.* **2023**, *6*, 19. [[CrossRef](#)]
34. Brandes, E.A.; Vivekanandan, J.; Tuttle, J.D.; Kessinger, C.J. Hail production in a northeastern Colorado thunderstorm. In Proceedings of the 27th Conference on Radar Meteorology, Vail, CO, USA, 9–13 October 1995; pp. 527–529.
35. Browning, K.A. The structure and mechanisms of hailstorms. In *Review of Hail Science and Hail Suppression*; American Meteorological Society: Boston, MA, USA, 1977; Monograph 38; pp. 1–48.
36. Dessens, J.; Sánchez, J.L.; Berthet, C.; Hermida, L.; Merino, A. Hail prevention by ground-based silver iodide generators: Results of historical and modern field projects. *Atmos. Res.* **2016**, *170*, 98–111. [[CrossRef](#)]
37. Hughes, P.; Wood, R. Hail: The white plague. *Weatherwise* **1993**, *46*, 16–21. [[CrossRef](#)]
38. Kumjian, M.R.; Lombardo, K. A hail growth trajectory model for exploring the environmental controls on hail size: Model physics and idealized tests. *J. Atmos. Sci.* **2020**, *77*, 2765–2791. [[CrossRef](#)]

39. Yin, L.; Ping, F.; Xu, H.; Chen, B. Numerical Simulation and the Underlying Mechanism of a Severe Hail-Producing Convective System in East China. *J. Geophys. Res. Atmos.* **2021**, *126*, e2019JD032285. [[CrossRef](#)]
40. Liu, X.; Min, K.; Sang, J.; Ma, S. Classification of Hailstone Trajectories in a Hail Cloud over a Semi-Arid Region in China. *Adv. Atmos. Sci.* **2023**, *40*, 1877–1894. [[CrossRef](#)]
41. Changnon, S.A.; Changnon, D.; Hilberg, S.D. Hailstorms across the nation: An atlas about hail and its damages. In *Illinois State Water Survey Contract Report CR-2009-12*; Illinois State Water Survey: Champaign, IL, USA, 2009.
42. Wieringa, J.; Holleman, I. If cannons cannot fight hail, what else? *Meteorol. Z.* **2006**, *15*, 659–670. [[CrossRef](#)]
43. Vivekanandan, J.; Tuttle, J.D.; Brandes, E.A. Observational and modeling considerations for multiparameter radar detection of hail. In Proceedings of the 26th International Conference on Radar Meteorology, Norman, OK, USA, 1 April 1993; Volume 525, pp. 525–527.
44. Changnon, S.A. The climatology of hail in North America. In *Review of Hail Science and Hail Suppression*; American Meteorological Society: Boston, MA, USA, 1978; Monograph 38; pp. 107–128.
45. Chen, G.T.J. A study on the upper-tropospheric cold vortices: Cases accompanying thunderstorms. In *Proceedings of the Conference on Weather, Radar and Flight Safety*; Civil Aeronautics Administration: Taipei, Taiwan, 1990; pp. 329–349.
46. Deng, Z.; Yang, M.; Jiang, L.; Zou, H.; Cheng, Z. Preliminary study of a mesosynoptic case in early spring. *Meteorol. Mon.* **1989**, *10*, 43–48.
47. Smith, S.B. The Mesoscale Effect of Topography on the Genesis of Alberta Hailstorms. Master's Thesis, McGill University, Montreal, QC, USA, 1986.
48. Li, X.; Zhang, F.; Zhang, Q.; Kumjian, M.R. Sensitivity of Hail Precipitation to Ensembles of Uncertainties of Representative Initial Environmental Conditions From ECMWF. *J. Geophys. Res. Atmos.* **2019**, *124*, 6929–6948. [[CrossRef](#)]
49. Skamarock, W.C.; Klemp, J.B.; Dudhia, J.; Gill, D.O.; Barker, D.M.; Wang, W.; Powers, J.G. A description of the Advanced Research WRF version 3. *NCAR Tech. Note* **2008**, *475*, 113.
50. Brown, T.M.; Pogorzelski, W.H.; Giammanco, I.M. Evaluating hail damage using property insurance claims data. *Weather Clim. Soc.* **2015**, *7*, 197–210. [[CrossRef](#)]
51. Changnon, S.A. The scales of hail. *J. Appl. Meteorol. Climatol.* **1977**, *16*, 626–648. [[CrossRef](#)]
52. Changnon, S.A. Data and approaches for determining hail risk in the contiguous United States. *J. Appl. Meteorol.* **1999**, *38*, 1730–1739. [[CrossRef](#)]
53. Sánchez, J.; Fraile, R.; De La Madrid, J.; Fuente, M.D.L.; Rodriguez, P.; Castro, A. Crop damage: The hail size factor. *J. Appl. Meteorol. Climatol.* **1996**, *35*, 1535–1541. [[CrossRef](#)]
54. National Oceanic and Atmospheric Administration (NOAA) Website. 2021. Available online: <http://www.spc.noaa.gov/climo/> (accessed on 10 June 2021).
55. Towery, N.G.; Changnon, S.A., Jr.; Morgan, G.M., Jr. A review of hail-measuring instruments. *Bull. Am. Meteorol. Soc.* **1976**, *57*, 1132–1141. [[CrossRef](#)]
56. Löffler-Mang, M.; Schön, D.; Landry, M. Characteristics of a new automatic hail recorder. *Atmos. Res.* **2011**, *100*, 439–446. [[CrossRef](#)]
57. Long, B.; Matson, R.J.; Crow, E.L. The hailpad: Materials, data reduction and calibration. *J. Appl. Meteorol. Climatol.* **1980**, *19*, 1300–1313. [[CrossRef](#)]
58. Changnon, S.A. Note on recording hail incidences. *J. Appl. Meteorol. Climatol.* **1966**, *5*, 899–901. [[CrossRef](#)]
59. Morgan, G.M., Jr.; Towery, N.G. On the role of strong winds in damage to crops by hail and its estimation with a simple instrument. *J. Appl. Meteorol. Climatol.* **1976**, *15*, 891–898. [[CrossRef](#)]
60. Palencia, C.; Castro, A.; Gaiotti, D.; Stel, F.; Vinet, F.; Fraile, R. Hailpad-based research: A bibliometric review. *Atmos. Res.* **2009**, *93*, 664–670. [[CrossRef](#)]
61. Kim, J.; Jang, K.I. Benefits of the next generation geostationary meteorological satellite observation and policy plans for expanding satellite data application: Lessons from GOES-16. *Atmosphere* **2018**, *28*, 201–209.
62. Yoon, K.H. The present and future state of national disaster prevention system in Korea. *J. Korean Soc. Environ. Eng.* **2008**, *30*, 128–135.
63. Kim, J.H.; Bae, D.H. A Study on Stochastic Radar Rainfall Estimation. In Proceedings of the Korea Water Resources Association Conference, Pyeongchang, Republic of Korea, 15–18 May 2007; pp. 311–315.
64. Féral, L.; Sauvageot, H.; Soula, S. Hail detection using S-and C-band radar reflectivity difference. *J. Atmos. Ocean. Technol.* **2003**, *20*, 233–248. [[CrossRef](#)]
65. Schmidt, M.; Tromel, S.; Ryzhkov, A.V.; Simmer, C. Severe hail detection: Hydrometeor classification for polarimetric C-band radars using fuzzy-logic and T-matrix scattering simulations. In Proceedings of the 2018 19th International Radar Symposium (IRS), Bonn, Germany, 20–22 June 2018.
66. López, L.; García-Ortega, E.; Sánchez, J.L. A short-term forecast model for hail. *Atmos. Res.* **2007**, *83*, 176–184. [[CrossRef](#)]
67. Snook, N.; Jung, Y.; Brotzge, J.; Putnam, B.; Xue, M. Prediction and ensemble forecast verification of hail in the supercell storms of 20 May 2013. *Weather Forecast.* **2016**, *31*, 811–825. [[CrossRef](#)]
68. Li, D.J.G.; McGovern, A.; Haupt, S.E.; Sobash, R.A.; Williams, J.K.; Xue, M. Storm-based probabilistic hail forecasting with machine learning applied to convection-allowing ensembles. *Weather Forecast.* **2017**, *32*, 1819–1840.

69. Kim, I.G. Premodern meteorological prediction reference and phenology structure on the Chosun Wisun-ji text. *Korean Stud. Q.* **2013**, *36*, 217–253.
70. Yu, W.S.; Yoon, S.S.; Choi, M.; Jung, K. Performance comparison of rainfall and flood forecasts using short-term numerical weather prediction data from Korea and Japan. *J. Korea Water Resour. Assoc.* **2017**, *50*, 537–549.
71. Manzato, A. Hail in northeast Italy: Climatology and bivariate analysis with the sounding-derived indices. *J. Appl. Meteorol. Climatol.* **2012**, *51*, 449–467. [[CrossRef](#)]
72. Adams-Selin, R.D.; Ziegler, C.L. Forecasting hail using a one-dimensional hail growth model within WRF. *Mon. Weather Rev.* **2016**, *144*, 4919–4939. [[CrossRef](#)]
73. Li, X.; Zhang, Q.; Xue, H. The role of initial cloud condensation nuclei concentration in hail using the WRF NSSL 2-moment microphysics scheme. *Adv. Atmos. Sci.* **2017**, *34*, 1106–1120. [[CrossRef](#)]
74. Li, X.; Zhang, Q.; Fan, J.; Zhang, F. Notable Contributions of Aerosols to the Predictability of Hail Precipitation. *Geophys. Res. Lett.* **2021**, *48*, e2020GL091712. [[CrossRef](#)]
75. Fan, J.; Zhang, Y.; Wang, J.; Jeong, J.H.; Chen, X.; Zhang, S.; Lin, Y.; Feng, Z.; Adams-Selin, R. Contrasting responses of hailstorms to anthropogenic climate change in different synoptic weather systems. *Earth's Future* **2022**, *10*, e2022EF002768. [[CrossRef](#)]
76. Púčik, T.; Castellano, C.; Groenemeijer, P.; Kühne, T.; Rädler, A.T.; Antonescu, B.; Faust, E. Large hail incidence and its economic and societal impacts across Europe. *Mon. Weather Rev.* **2019**, *147*, 3901–3916. [[CrossRef](#)]
77. Fiss, C.J.; McNeil, D.J.; Rodríguez, F.; Rodewald, A.D.; Larkin, J.L. Hail-induced nest failure and adult mortality in a declining ground-nesting forest songbird. *Wilson J. Ornithol.* **2019**, *131*, 165–170. [[CrossRef](#)]
78. McMaster, H. Hailstorm risk assessment in rural New South Wales. *Nat. Hazards* **2001**, *24*, 187–196. [[CrossRef](#)]
79. Cox, M.; Armstrong, P.R. A statistical model for the incidence of large hailstones on solar collectors. *Sol. Energy* **1981**, *26*, 97–111. [[CrossRef](#)]
80. Heymsfield, A.J.; Giammanco, I.M.; Wright, R. Terminal velocities and kinetic energies of natural hailstones. *Geophys. Res. Lett.* **2014**, *41*, 8666–8672. [[CrossRef](#)]
81. Cremer, K.W. Hail damage in Australian pine plantations I. Nature and extent of damage. *Aust. For.* **1984**, *47*, 103–114. [[CrossRef](#)]
82. Battaglia, M.; Lee, C.; Thomason, W.; Fike, J.; Sadeghpour, A. Hail damage impacts on corn productivity: A review. *Crop Sci.* **2019**, *59*, 1–14. [[CrossRef](#)]
83. Beal, A.; Hallak, R.; Martins, L.D.; Martins, J.A.; Biz, G.; Rudke, A.P.; Tarley, C.R.T. Climatology of hail in the triple border Paraná, Santa Catarina (Brazil) and Argentina. *Atmos. Res.* **2020**, *234*, 104747. [[CrossRef](#)]
84. Beresford, B.C. Effect of simulated hail damage on yield and quality of potatoes. *Am. Potato J.* **1967**, *44*, 347–354. [[CrossRef](#)]
85. Ferguson, H.; Jones, A.J.; Tsai, K.J. Damage to barley spikes resulting from impact momentum similar to small sized hail. *Agron. J.* **1987**, *79*, 1015–1018. [[CrossRef](#)]
86. Lim, Y.S.; Kim, M.K.; Park, S.H.; Woo, I.D.; Shin, Y.S.; Kim, S.J. Suggestion of standard for rebuilding according to the degree of hail damage of apple tree orchard. *Hortic. Abstr.* **2019**, *37*, 118–119.
87. Allen, J.T.; Tippett, M.K.; Sobel, A.H. An empirical model relating US monthly hail occurrence to large-scale meteorological environment. *J. Adv. Model. Earth Syst.* **2015**, *7*, 226–243. [[CrossRef](#)]
88. Hohl, R.; Schiesser, H.-H.; Aller, D. Hailfall: The relationship between radar-derived hail kinetic energy and hail damage to buildings. *Atmos. Res.* **2002**, *63*, 177–207. [[CrossRef](#)]
89. Höller, M.E.; Reinhardt, M.E. The Munich hailstorm of July 12, 1984—Convective development and preliminary hailstone analysis. *Beiträge Phys. Atmos.* **1986**, *59*, 1–12.
90. Charlton, R.B.; Kachman, B.M.; Wojtiw, L. Urban hailstorms: A view from Alberta. *Nat. Hazards* **1995**, *12*, 29–75. [[CrossRef](#)]
91. Andrews, K.E.; Blong, R.J. March 1990 hailstorm damage in Sydney, Australia. *Nat. Hazards* **1997**, *16*, 113–125. [[CrossRef](#)]
92. Laurie, J.A.P. Hail and its effects on buildings. In *CSIR Research Report No. 176; Bulletin 21; National Building Research Institute: Pretoria, South Africa, 1960*; pp. 1–12.
93. Morrison, S. Causes and extent of damage related to structure, material, and architectural failure. In *Hail, Hail the Disaster's Here; Employers Reinsurance Corp.: Overland Park, KS, USA, 1997*; p. 12.
94. Rhodes, K. Developing standards to evaluate impact resistance of roofing materials. In *Hail, Hail the Disaster's Here; Employers Reinsurance Corp.: Overland Park, KS, USA, 1997*; p. 5.
95. Marshall, T.; Herzog, R.; Morrison, S.; Smith, S. Hail damage threshold sizes for common roofing materials. In *Proceedings of the 21st Conference on Severe Local Storms, San Antonio, TX, USA, 11 August 2002*; Transactions of the American Meteorological Society: Washington, DC, USA, 2002; p. 3.
96. Teule, T.; Appeldoorn, M.; Bosma, P.; Sprenger, L.; Koks, E.; Moel, H.D. *The Vulnerability of Solar Panels to Hail*; Vrije Universiteit Amsterdam: Amsterdam, The Netherlands, 2019.
97. Mathiak, G.; Sommer, J.; Reil, F.; Althaus, J.; Kontges, M.; Nusperling, M. *Hail Impact on PV Module Reliability*; International Energy Agency: Munich, Germany, 2015.
98. Moore, D.; Wilson, A. *Photovoltaic Solar Panel Resistance to Simulated Hail*; Report DOE/JPL-1012-78/6; California Institute of Technology: Pasadena, CA, USA, 1978.
99. Allen, J.T.; Allen, E.R. A review of severe thunderstorms in Australia. *Atmos. Res.* **2016**, *178*, 347–366. [[CrossRef](#)]
100. Blamey, R.C.; Middleton, C.; Lennard, C.; Reason, C.J.C. A climatology of potential severe convective environments across South Africa. *Clim. Dyn.* **2017**, *49*, 2161–2178. [[CrossRef](#)]

101. Brooks, H.E.; Lee, J.W.; Craven, J.P. The spatial distribution of severe thunderstorm and tornado environments from global reanalysis data. *Atmos. Res.* **2003**, *67–68*, 73–94. [[CrossRef](#)]
102. Gensini, V.A.; Ashley, W.S. Climatology of potentially severe convective environments from the North American Regional Reanalysis. *Electron. J. Sev. Storms Meteorol.* **2011**, *6*, 1–15.
103. Ni, X.; Zhang, Q.; Liu, C.; Li, X.; Zou, T.; Lin, J.; Kong, H.; Ren, Z. Decreased hail size in China since 1980. *Sci. Rep.* **2017**, *7*, 10913. [[CrossRef](#)]
104. Kim, S.; Lee, S.-J.; Shim, K.M. Hail risk map based on multidisciplinary data fusion. *Korean J. Agric. For. Meteorol.* **2022**, *24*, 234–243, (In Korean with English abstract).
105. Marinică, I. *Fenomene Meteorologice Extreme in Oltenia (Extreme Meteorological Phenomena in Oltenia)*; MJM Press: Craiova, Romanian, 2003; p. 280.
106. Randalls, S.; Kneale, J. A Fragile Network: Effecting Hail Insurance in Britain, 1840–1900. *Enterp. Soc.* **2021**, *22*, 739–769. [[CrossRef](#)]
107. Sarvia, F.; De Petris, S.; Borgogno-Mondino, E. A methodological proposal to support estimation of damages from hailstorms based on Copernicus Sentinel 2 data times series. In *Lernational Conference on Computational Science and Its Applications. ICCSA 2020. In Lecture Notes in Computer Science*; Springer: Cham, Switzerland, 2020; Volume 12252, pp. 737–751.
108. Shin, D.H. Review of the compulsory storm and flood insurance and policy implications. *J. Insur. Financ.* **2008**, *54*, 77–107.
109. Diaz-Caneja, M.B.; Conze, C.G.; Dittmann, C.; Pinilla, F.J.G.; Stroblmair, J. *Agricultural Insurance Schemes*; Office for Official Publications of the European Union: Luxembourg, Luxembourg, 2008.
110. Enjolras, G.; Sentis, P. Crop insurance policies and purchases in France. *Agric. Econ.* **2011**, *42*, 475–486. [[CrossRef](#)]
111. Garrido, A.; Zilberman, D. Revisiting the demand of agricultural insurance: The case of Spain (No. 686-2016-47109). *Agric. Financ. Rev.* **2008**, *68*, 43–66. [[CrossRef](#)]
112. Finger, R.; Lehmann, N. The influence of direct payments on farmers' hail insurance decisions. *Agric. Econ.* **2012**, *43*, 343–354. [[CrossRef](#)]
113. Khudiyev, N.N.; Dadashov, A.A. Current status and socio-economic aspects of the agricultural insurance system in Azerbaijan. In *Economic and Social Development: Book of Proceedings*; Varazdin Development and Entrepreneurship Agency and University North: Rabat, Morocco, 2022; pp. 271–276.
114. Inshakova, O.; Uskova, M.S.; Dolinskaya, V.V.; Frolova, E.E. Dynamics of the legislative development of public-private partnership in the sphere of agricultural insurance in Russia and the US. *Rev. Espac.* **2018**, *39*, 2–9.
115. Naghshpour, S. Are exports an engine of growth? *Int. J. Trade Glob. Mark.* **2012**, *5*, 153–166. [[CrossRef](#)]
116. Changnon, S.A.; Ivens, J.L. History repeated: The forgotten hail cannons of Europe. *Bull. Am. Meteorol. Soc.* **1981**, *62*, 368–375. [[CrossRef](#)]
117. Solomakhin, A.; Blanke, M. Improving light conditions by use of reflective mulch cloth (ExtendayTM) in an apple orchard under hail nets. IX International Symposium on Integrating Canopy, Rootstock and Environmental Physiology in Orchard Systems. *Acta Hortic.* **2008**, *903*, 1101–1105.
118. Mariani, L.; Ferrante, A. Agronomic management for enhancing plant tolerance to abiotic stresses—Drought, salinity, hypoxia, and lodging. *Horticulturæ* **2017**, *3*, 52. [[CrossRef](#)]
119. Mészáros, M.; Béliková, H.; Čonka, P.; Náměstek, J. Effect of hail nets and fertilization management on the nutritional status, growth and production of apple trees. *Sci. Hortic.* **2019**, *255*, 134–144. [[CrossRef](#)]
120. Mupambi, G.; Anthony, B.M.; Layne, D.R.; Musacchi, S.; Serra, S.; Schmidt, T.; Kalcsits, L.A. The influence of protective netting on tree physiology and fruit quality of apple: A review. *Sci. Hortic.* **2018**, *236*, 60–72. [[CrossRef](#)]
121. Singh, N.P.; Bal, S.K.; More, N.S.; Singh, Y.; Gudge, A. Adaptation and intervention in crops for managing atmospheric stresses. In *Climate Change and Agriculture in India; Impact and Adaptation*; Springer: Cham, Switzerland, 2019; pp. 111–127.
122. Castellano, S.; Mugnozza, G.S.; Russo, G.; Briassoulis, D.; Mistriotis, A.; Hemming, S.; Waaijenberg, D. Plastic nets in agriculture: A general review of types and applications. *Appl. Eng. Agric.* **2008**, *24*, 799–808. [[CrossRef](#)]
123. Bosco, L.C.; Bergamaschi, H.; Cardoso, L.S.; de Paula, V.A.; Marodin, G.A.B.; Brauner, P.C. Microclimate alterations caused by agricultural hail net coverage and effects on apple tree yield in subtropical climate of Southern Brazil. *Bragantia* **2017**, *77*, 181–192. [[CrossRef](#)]
124. Salem, B.B. Arid zone forestry: A guide for field technicians. In *FAO Conservation Guide (20)*; FAO: Rome, Italy, 1989.
125. Pelley, J. Does cloud seeding really work. *Chem. Eng. News* **2016**, *92*, 18–21.
126. Morgan, G.M. The return of the anti-hail cannons. *Weatherwise* **2008**, *61*, 14–19. [[CrossRef](#)]
127. Čurić, M.; Janc, D.; Vučković, V. Cloud seeding impact on precipitation as revealed by cloud-resolving mesoscale model. *Meteorol. Atmos. Phys.* **2007**, *95*, 179–193. [[CrossRef](#)]
128. Hill, S.; Ming, Y. Nonlinear climate response to regional brightening of tropical marine stratocumulus. *Geophys. Res. Lett.* **2012**, *39*, L15707. [[CrossRef](#)]
129. Birsan, M.; Muscalu, A.; Voicea, I.; Pruteanu, A. General aspects of the extreme meteorological phenomenon: Hail. *Ann. Fac. Eng. Hunedoara Int. J. Eng.* **2019**, *17*, 81–88.
130. Mihailescu, C.; Radulescu, M. The study of the influence of propellant performances changes on the ballistic characteristics of anti-hail rocket. *Rev. Air Force Acad.* **2015**, *3*, 55–58. [[CrossRef](#)]
131. Morgan, G.M., Jr. A general description of the hail problem in the Po Valley of northern Italy. *J. Appl. Meteorol. Climatol.* **1973**, *12*, 338–353. [[CrossRef](#)]

132. Neyman, J.; Sansom, H. Rockets and hail. *Weather* **1966**, *21*, 336–337.
133. Davis, S.A.C., Jr.; Farhar, R.J.; Haas, B.C.; Ivens, J.E.; Jones, J.L.; Mann, M.V.; Morgan, D.; Sonka, G.M., Jr.; Swanson, S.T.; Taylor, E.R.; et al. *Hail Suppression Impacts and Issues. Final Report, Ill*; Illinois State Water Survey: Champaign, IL, USA, 1977; 441p.
134. Yuter, S.E.; Houze, R.A., Jr. Three-dimensional kinematic and microphysical evolution of Florida cumulonimbus. Part III: Vertical mass transport, mass divergence, and synthesis. *Mon. Weather Rev.* **1995**, *123*, 1964–1983. [[CrossRef](#)]
135. Houston, W. Severe hail damage to mangroves at Port Curtis, Australia. *Mangroves Salt Marshes* **1999**, *3*, 29–40. [[CrossRef](#)]

Disclaimer/Publisher’s Note: The statements, opinions and data contained in all publications are solely those of the individual author(s) and contributor(s) and not of MDPI and/or the editor(s). MDPI and/or the editor(s) disclaim responsibility for any injury to people or property resulting from any ideas, methods, instructions or products referred to in the content.